APPLICATIONS OF INSAR AND 2D SEISMIC INTERPRETATION FOR SALT TECTONIC STUDIES IN THE SALT RANGE AND POTWAR PLATEAU REGION, NORTHERN PAKISTAN

.....

A Thesis

Presented to

the Faculty of the Department of Earth and Atmospheric Sciences

University of Houston

.....

In Partial Fulfillment

of the Requirements for the Degree

Master of Science

.....

By

Ismail Ahmad Abir

December 2012

APPLICATIONS OF INSAR AND 2D SEISMIC INTERPRETATION FOR SALT TECTONIC STUDIES IN THE SALT RANGE AND POTWAR PLATEAU REGION, NORTHERN PAKISTAN

Ismail Ahmad Abir

APPROVED:

Dr. Shuhab D. Khan, Associate Professor
(Committee Chair)
Department of Earth and Atmospheric Sciences, University of Houston

Dr. Rebecca Bendick, Associate Professor
Department of Geosciences,
University of Montana

Dr. Craig Glennie, Assistant Professor
Department of Civil and Environmental Engineering, University of Houston

Dr. Jolante Van Wijk, Assistant Professor
Department of Earth and Atmospheric Sciences, University of Houston

Dr. Mark A. Smith, Dean, College of Natural Sciences and Mathematics,
University of Houston

ACKNOWLEDGEMENTS

Of the utmost importance, I would like to thank my advisor and teacher, Dr. Shuhab Khan, whom I have high respect and regards, for his tremendous patience and guidance during my work. I have learned a lot from him and sincerely appreciate his valuable advice which helped me to be a better researcher and person. Without his help and wisdom, this work would not have been possible.

My sincere gratitude goes to my committee members: Dr. Jolante Van Wijk, Dr. Craig Glennie, and Dr. Rebecca Bendick for providing insights and critically reviewing my thesis. I would also like to thank the professors in the Department of Earth and Atmospheric Sciences for their exciting lectures, especially Dr. Christopher Liner, Dr. Robert Stewart, Dr. John Castagna, Dr. Evgeny Chesnokov, and Dr. Aibing Li.

I would like to thank my friends and colleagues in the remote sensing lab for their help and support. They made my days at University of Houston fun and exciting. I would like to thank my good friend and colleague, Dr. Aziz Ozyavas for his help in InSAR. I also owe a lot to my friend and colleague, Yahaya Abubakar, for helping me with understanding the concept of geomorphic indices.

Grateful thanks to my family members, especially my parents, for their support and encouragement. However, not enough words can express my sincere gratitude towards my parents. I highly respect and value their sincere advice. Also, I would like to thank my brother, Ilyas, for his determination in his support for me.

APPLICATIONS OF INSAR AND 2D SEISMIC INTERPRETATION FOR SALT TECTONIC STUDIES IN THE SALT RANGE AND POTWAR PLATEAU REGION, NORTHERN PAKISTAN

.....

An Abstract of a Thesis

Presented to

the Faculty of the Department of Earth and Atmospheric Sciences

University of Houston

.....

In Partial Fulfillment

of the Requirements for the Degree

Master of Science

.....

By

Ismail Ahmad Abir

December 2012

ABSTRACT

Salt tectonics in Northern Pakistan affects the geological structures and the seismology of the area. Salt layers are important in influencing the deformation style of geological structures. The difference in deformation intensity between the Potwar Plateau-Salt Range and the Kohat Plateau-Surghar Range systems is attributed to the presence of a Pre-Cambrian salt layer. Overburden will translate efficiently on the ductile salt detachment and will result in low internal deformation, which is evident in the Potwar Plateau-Salt Range system. In this system, the salt layers act as a lubricant between the overlying sedimentary layers and the basement rocks. In contrast, the Kohat Plateau-Surghar Range system has high internal deformation. This could be due to the absence or the thinning of the salt layers which causes increase friction between the overburden and the basement rocks. This study is an attempt to investigate the role of salt in the geological deformation of the Salt Range-Potwar Plateau using InSAR, 2-D seismic interpretations, and geomorphic index calculations. 3-pass interferometry was done using 8 ALOS PALSAR scenes, in order to create a surface displacement map with two years temporal difference. The InSAR and geomorphic index results suggest that the Salt Range may still be active tectonically and has undergone uplift. Six migrated seismic reflection lines were interpreted showing basement ramps due to normal faults. These ramps are believed to act as transition zones between different roles of salt; salt layer act as a decollement to the north and salt flow is prominent to the south. Furthermore, the results also suggest that differential loading is the main driving force for the salt flowing to the south. However, buoyancy force may play a significant role in the deformation of

the Salt Range due to the uplift. Moreover, both the salt layer and the geometry of the basement influence the deformation style in this region. This thesis suggests that the Salt Range and Potwar Plateau region is a thin-skinned fold-and-thrust belt due to the wedge shape of the plateau and the salt as the weak detachment layer.

Table of Contents

LIST OF FIGURES

LIST OF TABLES

ABBREVIATIONS

ALOS	Advanced Land Observing Satellite
DEM	Digital Elevation Model
FBD	Fine Beam Double Polarization
FBS	Fine Beam Single Polarization
GPS	Global Positioning System
HH	Horizontal-Horizontal
HV	Horizontal-Vertical
InSAR	Interferometric Synthetic Aperture Radar
KF	Kalabagh Fault
LOS	Line of Sight
MBT	Main Boundary Thrust
MCT	Main Central Thrust
MFT	Main Frontal Thrust
NPDZ	Nothern Potwar Deformation Zone
PALSAR	Phased Array Type L-band Synthetic Aperture Radar
PP	Potwar Plateau
SAR	Synthetic Aperture Radar
SR	Salt Range
SRF	Salt Range Formation
SR-KP	Surghar Range-Kohat Plateau

SRTM	Shuttle Radar Topography Mission
VH	Vertical-Horizontal
VV	Vertical-Vertical

Chapter 1:

Introduction

1.1 Introduction

This thesis is an attempt to investigate the role of salt in the geologic deformation of the Salt Range-Potwar Plateau, which is located in Northern Pakistan, using mainly InSAR (Interferometric Synthetic Aperture Radar) and 2-D seismic interpretations (Figure 1.1 and Figure 1.2). Additionally, mountain-front sinuosity index was calculated for the Salt Range region. The main objectives of this study are to map the geological structures in the subsurface that may be caused by the salt layer in this region, using interpretations of 2-D seismic lines and attempts to understand the surface deformation of the Salt Range using InSAR. By combining results from both the surface (InSAR and geomorphic index) and the sub-surface (seismic), the movements of the region as well as the driving force for the salt are investigated.

1.2 Overview

The northwestern Himalaya has undergone intense deformation due to compressional forces between the subducted Indian plate and the Eurasian plate (Thakur, 2004; Chen and Khan, 2010; Yin, 2006). Four Cenozoic fault systems that are dipping north were created, which are the Main Frontal Thrust (MFT), Main Boundary Thrust (MFT), Main Central Thrust (MCT), and the South Tibetan Detachment System (STDS) (Yin and Harrison, 2000; Hodges, 2000). These thrust systems were created to accommodate the shortenings in the Sub-Himalayas. As the shortening progresses, new faults were generated southward (Leathers, 1987).

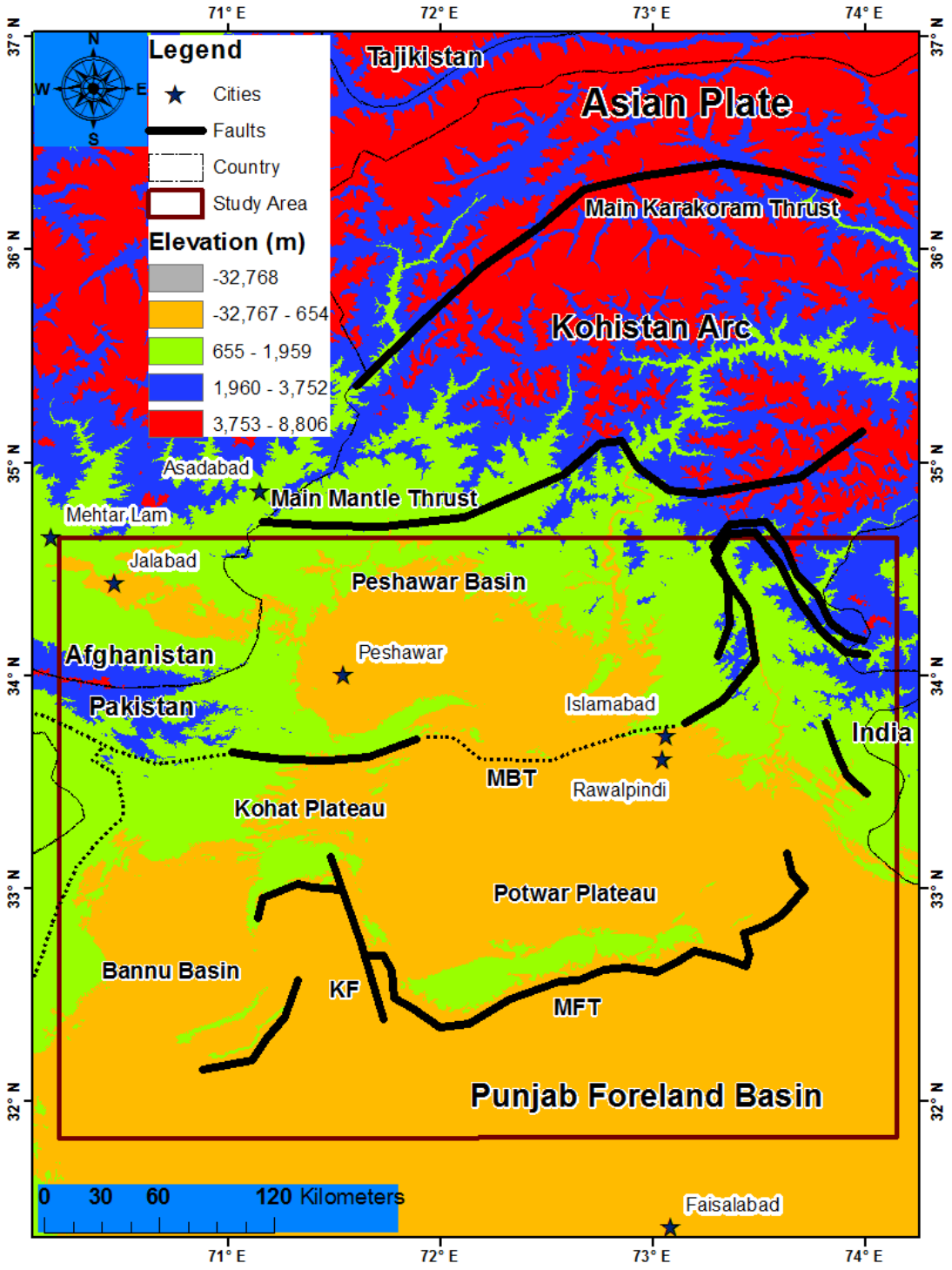

Figure 1.1: A geological map showing the main fault systems in Northern Pakistan. MFT is the Main Frontal Thrust; MBT is the Main Boundary Thrust; KF is the Kalabagh fault, which is a right-lateral strike-slip fault (Modified from Pivnik, 1992)

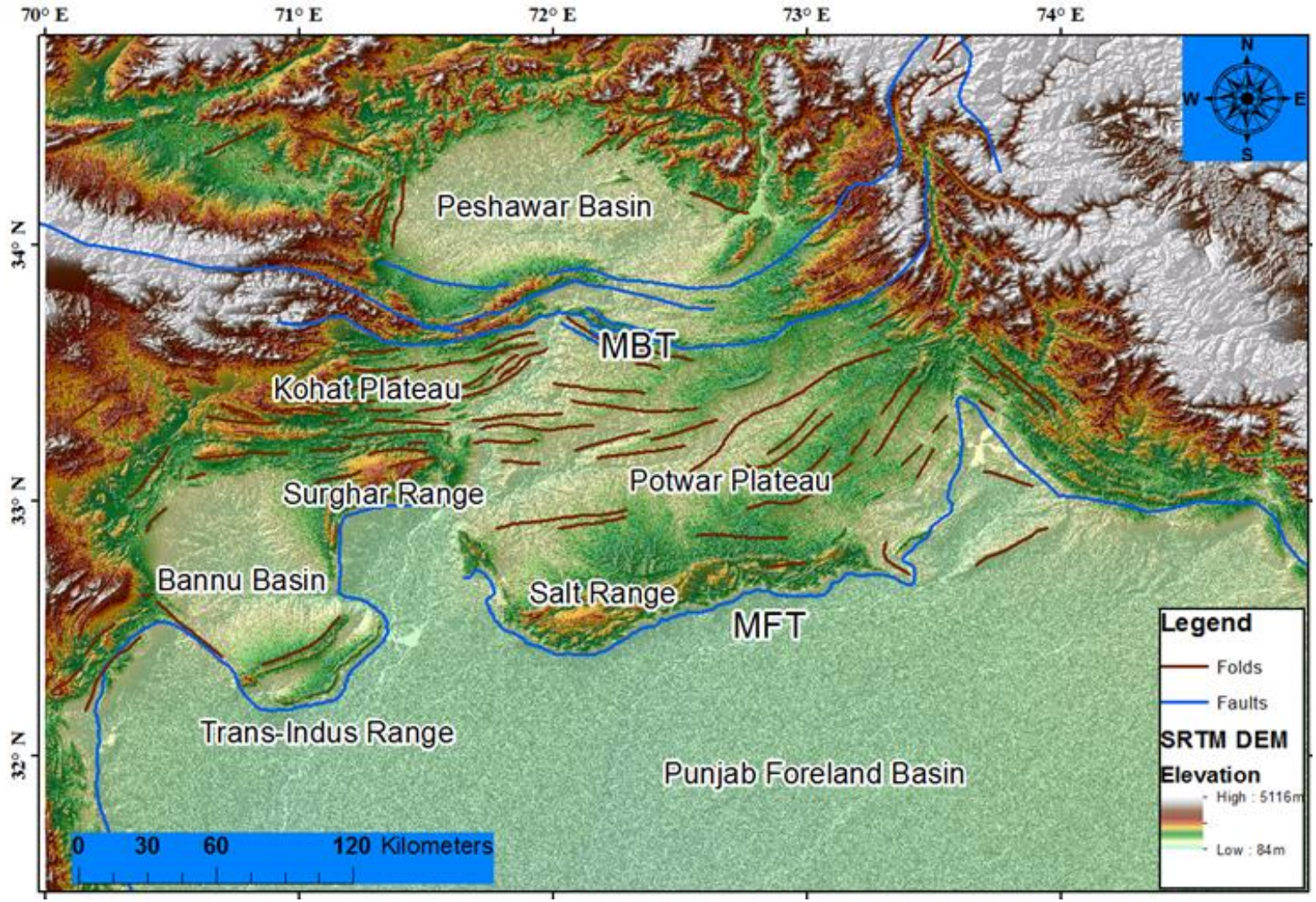

Figure 1.2: Map of the study area in Northern Pakistan. MBT is the Main Boundary Thrust and the MFT is the Main Frontal Thrust. The Salt Range-Potwar Plateau region is located between the MBT to the north and the MFT to the south.

Many folds and thrust faults characterize the intensity of the deformation, especially in the area between the MBT and the MFT, which is located in northern Pakistan (Figure 1.2). This system of folds and thrusts is called the fold-and-thrust belt. The intensity of deformation is not uniform across the area, which can be contributed to many factors, such as the lateral variations in the rheology of the detachments (Cotton and Koyi, 2000). In this area, the Late Pre-Cambrian salt layer (Salt Range Formation) plays an important role as the decollement of the overlying sedimentary layers (Robion et al., 2007). The Salt Range is an example of a major cratonic salt basin (Hudec and Jackson, 2007); its thickness varies from 500 meters to 1000 meters (Grelaud et al., 2002). As a result of the thick and ductile salt layers, the overlying strata may move more efficiently which may lead to less deformation (Robion et al., 2007). This can be seen clearly in the variation of the extent of the MFT between the Potwar Plateau-Salt Range (SR-PP) and the Kohat Plateau-Surghar Range (SR-KP) systems (Figure 1.2). In the Potwar-Plateau system, the MFT moved more southwardly as it slides on the Salt Range Formation (Figure 1.1 and Figure 1.2). The low coupling between the sliding overburden and the basement rock, which may be due to the salt detachment, leads to less internal deformation as well as a low taper angle (Cotton and Koyi, 2000). In contrast, the Kohat Plateau is more deformed and has a higher taper angle, which is believed to be attributed to the thinning or lack of salt in the region (Cotton and Koyi, 2000; Satyabala et al., 2012).

The difference in the deformation intensity between the Potwar-Plateau and Kohat Plateau systems resulted in the formation of the Kalabagh fault, which is a right-lateral

strike-slip fault. A detailed study of the Kalabagh Fault using remote sensing techniques, such as InSAR, has been done by Chen and Khan (2010). They found that the internal deformation of the Potwar Plateau is greater than at the front of the thrust. Numerous studies have focused on the Pre-Cambrian salt layer of the Salt Range (Yeats et al., 1984; Cotton and Koyi, 2000; Jaume and Lillie, 1988; Khan et al., 2012).

Other than influencing deformation intensity, the salt layer is found to affect seismicity. For instance, the Salt Range is a historically low seismicity area, which may be due to weak coupling between the salt decollement and the base rock (Yeats et al., 1984). In a study by Yeats and Lillie (1991), the earthquake history between Pakistan (SR-PP system) and northwestern Himalaya of India was compared. They suggested that the absence of big earthquakes in Pakistan, when compared to India, could be due to the existence of salt layer detachment in Pakistan. If this is true, then the folds and faults should undergo creep and aseismic growth to release the stored energy, which has not been observed (Yeats and Lillie, 1991). Furthermore, if the salt layer thins out north of the MBT, the area could be locked, and strain may be building up for a large earthquake (Yeats and Lillie, 1991). The MBT has three populated cities in its surrounding region (Islamabad, Rawalpindi and Peshawar), which accounts for around 4.1 million in population (Figure 1). A 2005 Kashmiri earthquake with a magnitude of 7.6 has occurred to the northeast of the study area close to the MBT, which devastated the area (Kaneda et al., 2008). Around 75,000 people died in that earthquake.

Additionally, the Potwar Plateau-Salt Range and the Kohat-Surghar systems are important areas for hydrocarbon production in Pakistan. The South Potwar Basin for

example hosts productive petroleum accumulations (Grelaud et al., 2002; Sercombe et al., 1998) (Figure 1.2). Therefore, the question of how salt layers deform and produce petroleum traps, such as anticlines, is essential, as around 60% of the world's hydrocarbon reserves are located within traps that are related to salt structures (Aftabi et al., 2010). Hence, studying the pattern and rate of flow for the salt layers will have advantages to both the study of neo-tectonics and the exploration of hydrocarbons in this area.

1.3 Role of Salt

Salt layers have a number of unique characteristics that makes them the "weak-link" in the deformation of geological layers (Jackson, 1995; Hudec and Jackson, 2007). One of them would be the fact that salt is, most of the time, less dense than the surrounding rocks. Therefore, at depth, these layers are buoyant, and tend to move upwards through any cracks or weaknesses in the overburden. Salt layers are ductile layers that may flow horizontally in the sub-surface as they try to reach the surface. This is mainly due to differential loading and the low density of salt (Hudec and Jackson, 2007; Jackson, 1995). According to Hudec and Jackson (2007), there are two factors that resist salt flow: the strength of overburden and the friction along the boundary of the salt body. In order for salt to flow, the driving forces must overcome these two factors. As the salt layer flows, it will deform and change the geological structures of the area. It is important to understand whether the flow of salt is deforming the geologic layers or whether the deformation of the layers is affecting the flow of salt. Due to these two main

characteristics, salt tectonic studies are important in understanding the deformation of a geological formation, especially in the fold-and–thrust belt of Northern Pakistan.

Many previous studies of the area have concluded that salt plays an important role in the tectonics of this area and mainly acts as a decollement or a detachment for the overlying sedimentary layers (Jaume, 1986; Jaume and Lillie, 1988). The salt layers act as a lubricant where the overburden can slide and creates a thrust fault called the Main Frontal Thrust (MFT). Due to the lateral difference in the salt layers across the study area, the movement of the overburden is affected. One clear example of this is the big contrast in the southward propagation of the MFT between the Salt Range-Potwar Plateau system and the Surghar Range-Kohat Plateau system, which resulted in the dextral strike-slip Kalabagh fault (Chen and Khan, 2010).

There are also exposed salt and salt domes in the study area, which are mainly located near the MFT. These salt structures affect the deformation differently, with mostly buoyancy and differential loading forces playing a significant role. Previous studies show that most of the structural deformation is concentrated at the edge of the belt, near the MFT (Lille et al., 1987; Cotton and Koyi, 2000).

1.4 Previous Studies

In order to understand the role of salt in the deformation style when compared to the Surghar Range-Kohat Plateau system, many studies have focused on the Salt Range-Potwar Plateau (SR-PP) region using a variety of geophysical techniques (Cotton and Koyi, 2000; Chapple, 1978; Davis and Engelder, 1985; Satyabala et al., 2012). Seismic

sections have been analyzed and interpreted for the western and eastern part of the Salt Range (Pennock, 1988; Chen, 2009; Khan et al. 2012). In this study, the seismic sections of central Salt Range are interpreted and compared with previous studies, in order to better understand the subsurface structures of the region. Furthermore, InSAR and GPS data have been used to study the surface movement in the region. In a study by Satyabala et al. (2012), InSAR was used to study the movement of the Surghar Range-Kohat Plateau area (SR-KP), which is adjacent to the SR-PP system. They concluded that the movement of the Kohat Plateau is similar to that of a caterpillar and argues that due to the thinning or lack of salt in this region, increasing friction between the overburden and the basement rock could accumulate stress and energy. This immense energy can result in a devastating earthquake. Therefore, the movement of the overburden is not consistent over time, but stalls as energy is stored and moves as energy is released. Can the same be said about SR-PP?

Other models that explain the deformation mechanisms in northwest Pakistan include the wedge model (Chapple, 1978) and the parallel strike-slip fault model (Treloar et al., 1992). The wedge model states that the overburden is wedge-shaped with thicker layers at the back of the thrust and the wedge is sliding over a basement rock. A detachment layer is located between the overburden and basement rock. In contrast, the parallel strike-slip model states that the Kalabagh fault is part of en echelon strike-slip faults that are parallel to the Chaman fault. More importantly, a study by Mcdougall and Khan (1990) suggests that the variation in the basement plays a more important role in deforming the fold-and-thrust belt than variation in the salt. In order to see which of these

models closely explains the deformation mechanism of this region, this study uses InSAR and seismic data.

Several modeling studies have addressed the role of salt layers as a decollement in fold-and-thrust belts, particularly the Salt Range and Potwar Plateau area (Cotton and Koyi, 2000; Chapple 1978). According to a study by Cotton and Koyi (2000), the lateral variation of the salt detachment is the main factor in influencing the propagation of the overlying sediments to the south. Their modeling study focused on the thickness of the salt layer as well as the thickness and the slope of the overburden. This east-west lateral variation includes the thickness of salt layer, thickness of overburden and the slope of overburden. Also, InSAR has been used to calculate the slip rate of the Kalabagh fault in a study (Chen and Khan, 2010).

1.5 Geological Framework

The study area is bounded on the north by the MBT and in the south by the MFT, where active thrusting is still occurring (Figure 1.1 and Figure 1.2). The crustal shortening in the area is due to the compression between the Indian plate and the Eurasian plate, which resulted in many thrust faults and folds in the area. Three main systems are located along the MFT, which are the Salt Range-Potwar Plateau, the Surghar Range-Kohat Plateau and the Trans-Indus Range-Bannu Basin. This study focuses on the Salt Range-Potwar Plateau region.

1.5.1 Salt Range-Potwar Plateau (SR-PP)

The SR-PP system is characterized by thick Pre-Cambrian salt layers. After the deposition of the Siwalik layers, the Salt Range area went through folding, thrusting and strong uplift (Yeats et al., 1984). In addition, the sub-surface data have shown that the SR-PP fold-and-thrust belt is thin-skinned, which means that the deformation does not involve the basement and only occurs in the cover rocks (Yeats and Lillie, 1991; Baker et al., 1988). The presence of the salt layers at the detachment is the main factor for the low internal deformation for this system. The four distinct parts of this system are the North Potwar deformation zone (NPDZ), the Soan Syncline, the Southern Potwar Plateau and the Salt Range (Cotton and Koyi, 2000). This system is bounded by two thrust systems, which are the MBT to the north and the MFT to the south. The dextral Kalabagh fault bounds the system to the west (Chen and Khan, 2010; McDougall and Khan, 1990; Treloar et al., 1992).

Moreover, this region has low seismicity, compared to both the Indian Sub-Himalayas and the Kohat Plateau region, due to the low coupling between the overburden and the basement rock (Yeats et al., 1984; Yeats and Lillie, 1991). This strongly suggests that the salt is concentrated mainly in the Potwar Plateau region.

The mechanisms that control the movement of the fold-and-thrust system includes the nature of the decollement, the taper angle and the compressional forces (Davis et al., 1983). The analogy of the mechanism is like the bulldozer wedge model by Davis et al. (1983). In this particular system, the decollement is the salt layer and due to its

incompressible nature, most of the Potwar Plateau was translated southward without much deformation. However, a majority of the deformation is concentrated near the southern edge of the system, where the overburden is pushed over the Punjab Foreland Basin.

Lillie et al. (1987) explain that the deformation style is different for the western, central, and eastern parts of the Salt Range. They suggested that the uplift of the Central Salt Range is attributed to a normal fault ramp in the basement rock. Due to the southward movement of the Potwar Plateau, the salt layer and the overburden are pushed over the ramp. Therefore, the thickest part of the salt is located in Salt Range.

1.5.2 Kohat Plateau-Surghar Range

The Surghar Range is the deformational front for the Kohat Plateau. Some have suggested that the Kohat Plateau has two detachments, which are the shallower Eocene evaporites (1.5-2 km deep) and the deeper Pre-Cambrian salt layer (6-7 km deep) (Abbasi and McElroy, 1990). The deformation of this system is influenced by the diapirism of the Eocene evaporates (Abbas and McElroy, 1990). Furthermore, the Kohat Plateau is more deformed than the Potwar Plateau. This may be attributed to the lack or thinning of salt in Kohat Plateau (Jaume, 1986; Baker et al. 1988).

1.5.3 Bannu Basin-Trans-Indus Range

The Trans-Indus Range is the deformational front for the Bannu Basin. The Trans-Indus Range extends most to the south compared to the Surghar Range and the Salt

Range. Moreover, the Trans-Indus Range is composed of two smaller sub-parallel ranges, which are the Marwat Range and the Khisor Range.

1.6 Stratigraphy

The stratigraphy of this region can be categorized into four main layers, which are, from the surface, the molasse (Siwalik and Rawalpindi), the carbonate platform, the Salt Range Formation and the basement rock (Figure 1.3). The Pre-Cambrian basement rock is a combination of igneous and metamorphic rocks of the Indian Shield (Pennock, 1988). The Salt Range Formation (SRF) is the oldest layer after the basement rock. This evaporite acts as a decollement for the overburden and varies in thickness in the region. Many evidences suggested that the salt is confined to the Potwar Plateau-Salt Range region, where the salt is likely to be deposited in isolation as discussed by Kozary et al. (1968).

Overlying the SRF is the carbonate platform, which is the hydrocarbon reservoir for this region. The platform ranges in age from Cambrian to Eocene, and consists of mainly limestone, shale, and sandstone (Pennock, 1988). There are multiple unconformities separating the Cambrian, Permian, and Paleocene-Eocene sections.

Above the platform is the molasse section, which consists the Miocene Rawalpindi Group and the Pliocene Siwalik Group. These layers are mainly sandstone and claystone. The Rawalpindi Group is divided into the Murree and the Kamlial, while the Siwalik Group is divided into the Chinji, the Nagri, and the Soan.

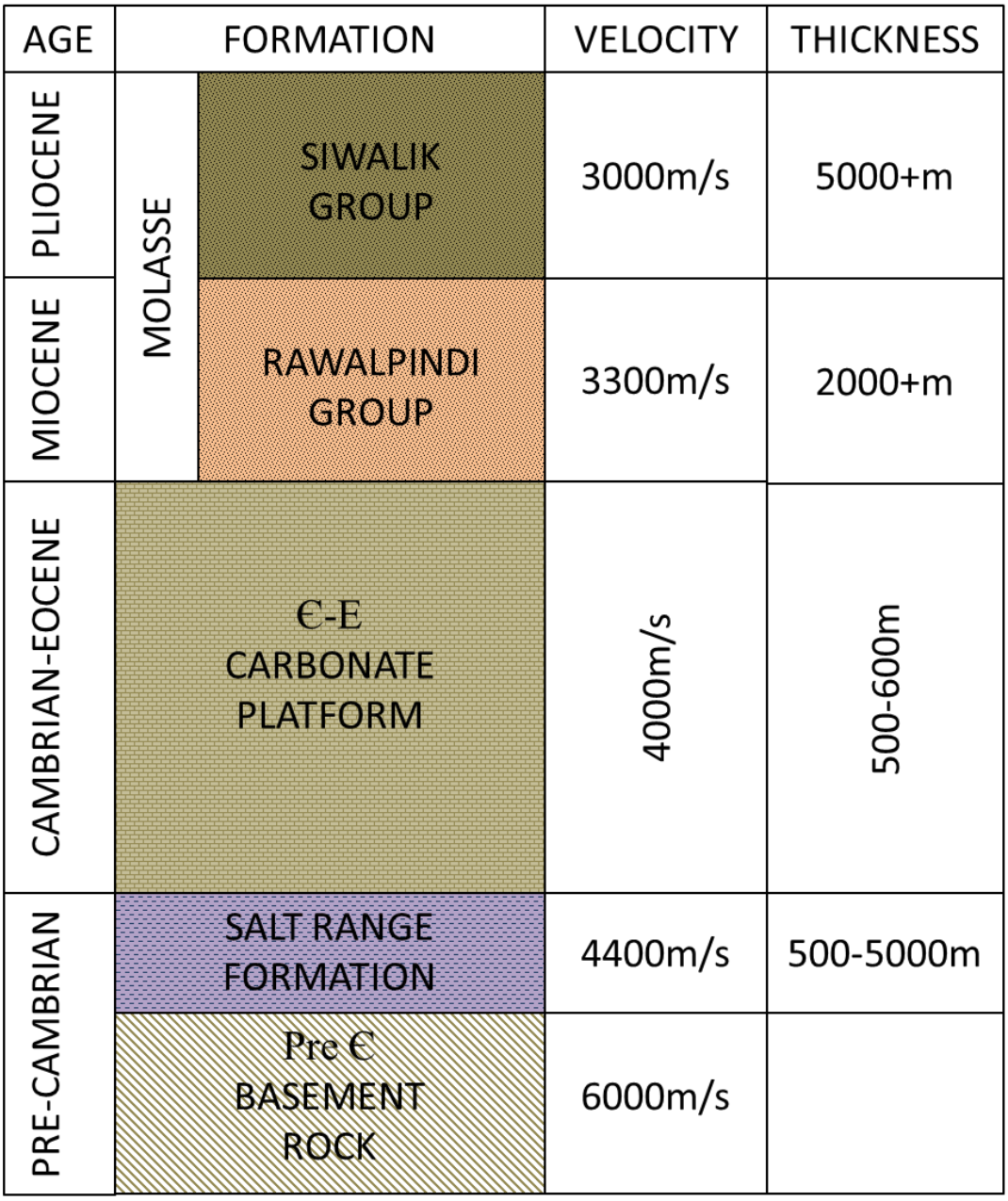

Figure 1.3: A generalized stratigraphic column of the SR-PP region. The stratigraphy of this region is consist of a molasse section followed by the carbonate platform, the Salt Range Formation and finally, the basement rock (Modified from Pennock, 1988)

1.7 Objectives

This work focuses on the Pre-Cambrian salt layer and its major impact on the tectonic of northwestern Pakistan by using the approach of backward modeling, in which a model is achieved through the mapping of the study area. Two methods are used in this study: the surface deformation of the western Salt Range and Potwar Plateau region is mapped using InSAR (Interferometric Synthetic Aperture Radar); and the subsurface geological structures as well as the Pre-Cambrian salt layer are mapped using geophysical techniques, mainly 2-D seismic interpretation. By using these tools, the flow and the role of salt can be interpreted.

1. InSAR is used to map the surface deformation of the study area. Two SAR (Synthetic Aperture Radar) images of different dates are compared, in order to calculate the difference in surface movements. ALOS PALSAR scenes are used for InSAR processing.

2. Migrated seismic lines located in Central Potwar Plateau are interpreted, in order to see the subsurface geology, especially any salt-related structures. The depth to the salt, the thickness of the salt and the basement layer are also be interpreted using seismic.

3. Mountain-front sinuosity is calculated for western Salt Range in order to detect any uplift in the region.

1.8 Methodology

In order to study the Pre-Cambrian salt in this area, three data sets are utilized; InSAR, 2-D seismic data and geomorphic indices. Furthermore, the 2-D seismic data are analyzed and interpreted to map the salt layer.

1.8.1 InSAR (Interferometric Synthetic Aperture Radar)

InSAR is a very powerful tool that can measure the movement and displacement of the surface very accurately. InSAR has been used to map and model a salt dome in Iran (Aftabi et al., 2010). Also, InSAR has also been used to study the displacement of the Kalabagh fault between the Potwar-Salt and the Kohat-Surghar systems (Chen, 2010).

SAR is an active remote sensing tool, where microwave energy is sent by the satellite towards the earth. Interferometry uses the difference in the phase between the outgoing signal and the incoming signal. By comparing two SAR images taken of the same area but at different times, we can measure the difference in their phase. The result is called the interferogram and shows information about range distance (Chen and Khan, 2010). Finally, we can find the line of sight (LOS) displacement between the two SAR images. ENVI Sarscape software is used for InSAR processing.

1.8.2 2D-Seismic Data

2-D seismic data from multiple seismic lines were obtained. These line are oriented approximately north-south/east-west and are located on the central part of the Potwar Plateau. Three additional lines, oriented north-south, were obtained and are

located near the MBT. These lines were interpreted using the seismic interpretation software SMT Kingdom. The results are compared with other published studies of seismic interpretation from other parts of the region.

1.8.3 Mountain-front Sinuosity

Mountain-front sinuosity is a method of geomorphic indices that calculates the relative active tectonic in the study area. This index is used to observe whether the Salt Range is uplifting or otherwise.

1.9 Outline of Chapters

This thesis consists of four chapters. The first chapter introduces the topic of salt tectonics in Northern Pakistan. It explains the main forces that influence the deformation of the study area and the important role that salt layers play. This chapter also sets the geological framework of the study area as well as the structure and stratigraphy of the Salt Range-Potwar Plateau region. Chapter 2 focuses on the datasets used and the methodology in processing the data. This chapter is basically divided into three parts, which are InSAR, 2-D seismic, and mountain-front sinuosity. Chapter 3 displays the results of all the datasets. The results include a displacement map using 3-pass interferometry technique, six interpreted lines and calculations of mountain-front sinuosity. Finally, Chapter 4 will discuss and summarize the results and interpretations of this thesis.

Chapter 2:

Data and Methodology

2.1 Introduction

This study utilizes three different datasets, which are Interferometry Synthethic Aperture Radar (InSAR), 2D seismic lines, and geomorphic indices. InSAR is a geophysical remote sensing technique that measures surface deformation of large areas with millimeters to centimeters accuracy (Li et al., 2007). This is a more efficient and less costly method compared to GPS (Global Positioning System). GPS stations have to be installed in the field and can be challenging especially in remote areas and regions with rugged terrain. In contrast, InSAR uses satellite images that can be acquired over any terrain in the world. Furthermore, radar signals are not affected by clouds or time of the day. Due to its versatility, InSAR has been applied to many studies, such as volcano monitoring (Massonnet et al.,1995; Hooper et al., 2004), fault slip rate measurement (Chen and Khan, 2010; Wright et al., 2004; Wang et al., 2009), land subsidence detection (Buckley et al., 2003; Motagh et al., 2007; Lubis et al., 2011), salt tectonic studies (Aftabi et al., 2010; Closson et al., 2011), and earthquake modeling (Weston et al., 2012). However, one of the limitations of InSAR is the lack of available SAR (Synthetic Aperture Radar) images for a particular study area. This thesis work used InSAR to investigate the surface movements of the western part of Salt Range and Potwar Plateau. By analyzing the pattern of the deformation, it is hoped to understand the movement of salt in the subsurface.

In a previous study by Aftabi et al. (2010), InSAR was used effectively to measure salt flow of an exposed salt diapir named Syahoo in Iran. Similarly, the

subsidence and uplift of the Lisan diapir was measured using InSAR (Closson et al., 2011). Movement of salt in the subsurface will have an effect on the surface. For instance, in an area where salt is flowing out, the overburden will fill the emptied space and subsidence will occur. In contrast, uplift will occur in areas where salt is filling the subsurface. This is important as we are trying to answer the question of whether salt layers in this region are acting mainly as a decollement or are causing the deformation by flowing. The 2D seismic lines will help in understanding the geological structures of the subsurface. The subsurface structures will be very useful in determining if the area is dominated by salt structures, which may indicate salt flow.

Geomorphic indices are parameters that show the relative movement of a particular region. In this work, one geomorphic index (mountain-front sinuosity) is used to calculate whether the region of Salt Range is uplifting. This chapter will explain the datasets that were used as well as the methods for the results obtained.

2.2 InSAR (Interferometry Synthetic Aperture Radar)

2.2.1 Datasets

Eight ascending Phased Array type L-band Synthetic Aperture Radar (PALSAR) scenes from the Advanced Land Observing Satellite (ALOS) were processed, with dates from January 2007 to August 2009 (Table 2.1). ALOS is a Japanese Earth satellite that was launched on January 24, 2006. It is a sun-synchronous satellite and has a repeat orbit cycle of 46 days. The PALSAR images obtained are in the fine resolution observation

Number	File Name	Date (mm/dd/yyyy)	Polarization	PALSAR Beam Mode
1	alpsrp191770640	8/30/2009	HH/HV	FBD
2	alpsrp158220640	1/12/2009	HH	FBS
3	alpsrp124670640	5/27/2008	HH/HV	FBD
4	alpsrp111250640	2/25/2008	HH	FBS
5	alpsrp104540640	1/10/2008	HH	FBS
6	alpsrp084410640	8/25/2007	HH/HV	FBD
7	alpsrp057570640	2/22/2007	HH	FBS
8	alpsrp050860640	1/7/2007	HH	FBS

Table 2.1: List of the ALOS PALSAR images used for processing using the InSAR technique. Scenes under the Fine Beam Single (FBS) mode have only Horizontal-Horizontal (HH) polarization. In contrast, scenes with Fine Beam Double (FBD) mode have Horizontal-Horizontal (HH) and Horizontal-Vertical (HV) polarization.

mode with the off-nadir angle of 34.3 degrees. Fine Beam Single Polarization (FBS) and Fine Beam Double Polarization (FBD) are the two types of fine resolution observation mode. Three of the scenes are in FBD, while the rest are in FBS (Table 2.1). In FBS mode, the PALSAR sensor only records single polarized data (HH or VV), while under FBD mode, it records double polarized data (HV or VH). Single polarized sensor (HH-Horizontal-Horizontal, VV-Vertical-Vertical) sends and receives radar signal of the same polarization. In contrast, double polarized sensor (HV-Horizontal-Vertical, VH-Vertical-Horizontal) sends and receives opposite polarized signals. For InSAR processing, only the HH polarization images were used. These images were downloaded from the Alaskan Satellite Facility-Distributed Active Archive Center (ASF-DAAC).

Figure 2.1 shows the location of the scenes, which covers the western end of Salt Range and southwest of the Potwar Basin. These images were selected due to their availability as well as their high number of repeat InSAR observations. Compared to other Synthetic Aperture Radar (SAR) satellites, ALOS PALSAR uses L-band wave, which is a larger wavelength (approximately 23.5cm) (Massonet and Feigl, 1998). SAR satellites also receive and transmit radar signals in other wavelengths; X-band wave (3cm), C-band wave (6cm), S-band wave (10cm), and P-band wave (65cm) (Massonet and Feigl, 1998). The usage of SAR images greatly depends on the penetration of the signal through vegetation or soil. As L-band signal has a longer wavelength, it can penetrate through dense vegetation in the study area and reach the surface.

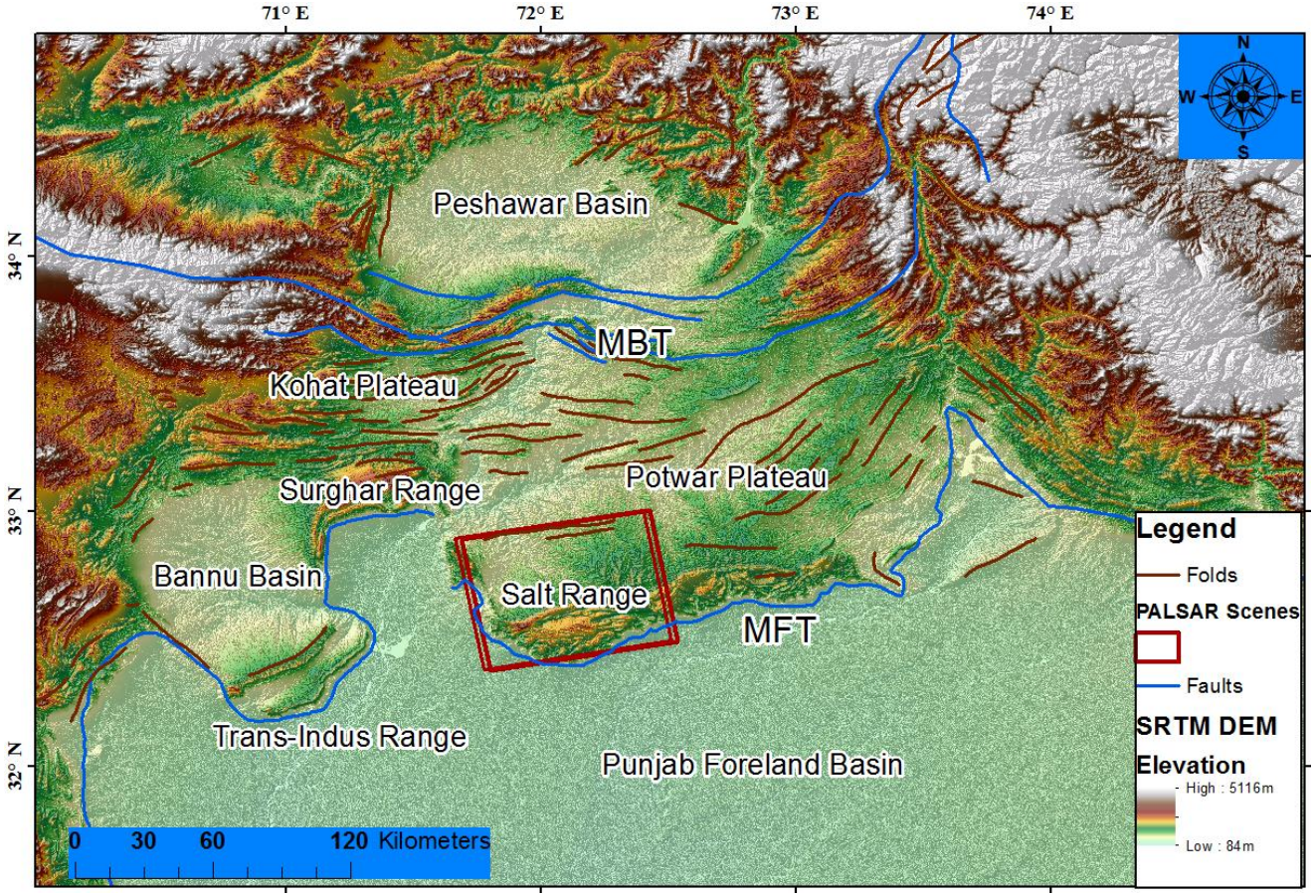

Figure 2.1: A topography map of the study area generated from SRTM 90m DEM. The red rectangles are the locations of the ALOS PALSAR scenes that were used in InSAR processing. The two main north-dipping thrust fault systems in the area are the MBT (Main Boundary Thrust) and the MFT (Main Frontal Thrust)

In order to use InSAR, at least two scenes are needed, called Master and Slave images. Both of the scenes are required to be from the same satellite platform and are taken from two different times over the same region (Figure 2.2).

From the 8 scenes that were obtained, 7 interferograms were created and the pairs with the lowest baseline and the largest temporal difference were selected (Table 2.2). Small perpendicular baseline (< 500m) is required for the pair to have high correlation, which is good for the unwrapping of interferograms. Ideally, both of the images should have zero perpendicular baselines. However, due to the low availability of the PALSAR scenes, the pairs that minimize the baseline were selected. Moreover, long temporal difference is ideal in order to detect the low surface deformation in this region. 3-pass interferometry was used to create a displacement map. The best pair that was selected for further processing that has a temporal difference of approximately two years (Table 2.2). A coherence map was created from the interferogram which shows the accuracy of the final results.

2.2.2 Principle of Interferometry

Synthetic Aperture Radar is an active remote sensing technique. Radar, which is an acronym for Radio Detection and Ranging, is consists of three main principles (ENVI, 2010). Firstly, the Radar sensor has to transmit microwave signal to the earth. The Radar sensor is mounted on a satellite, such as ALOS. Secondly, the sensor, which also acts as a receiver, records the reflected signal. Finally, the sensor records the strength (amplitude) and the time delay (phase) of the signal. Furthermore, the spatial resolution of the

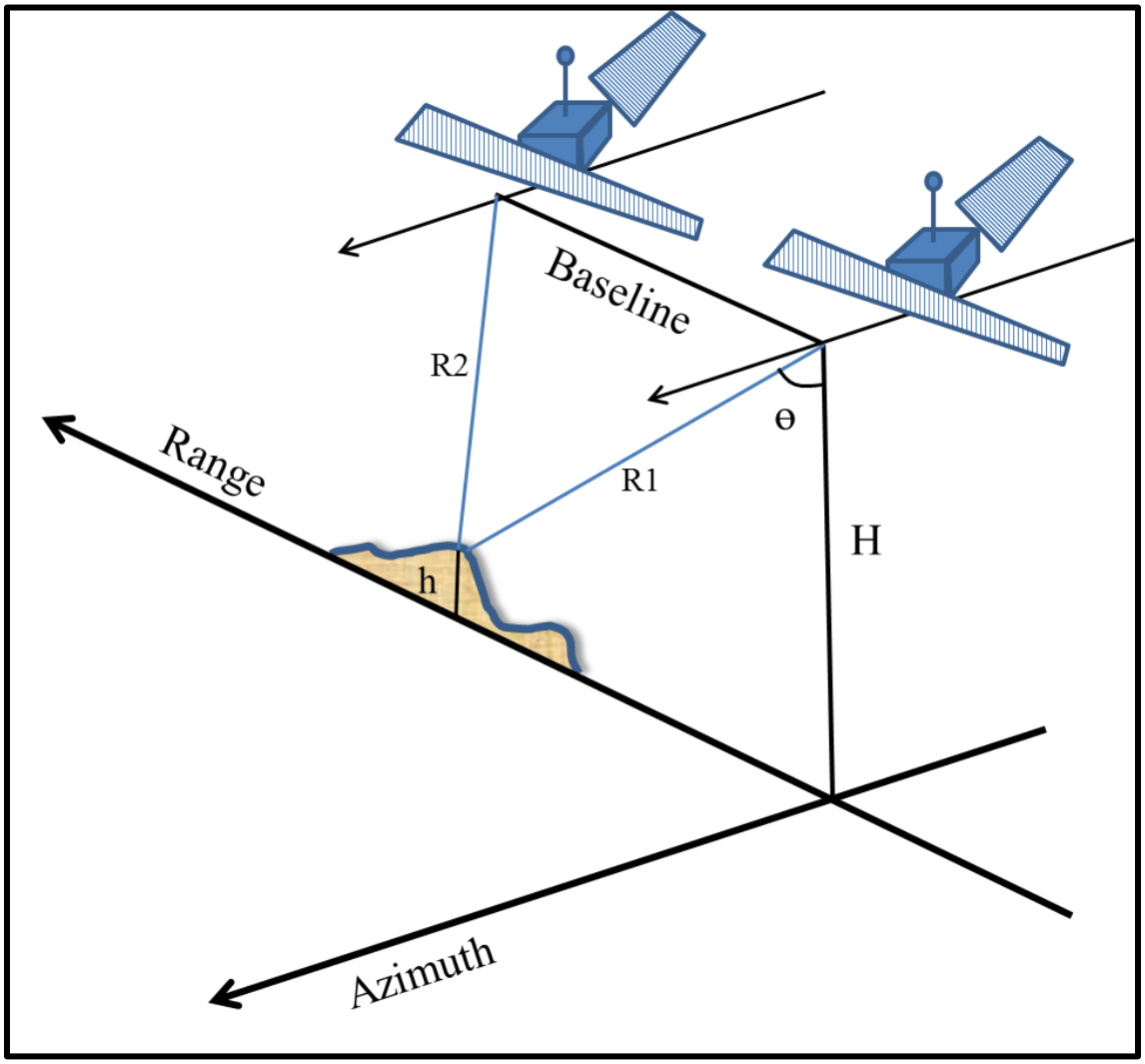

Figure 2.2: Basic concept of the principles of InSAR. Two repeat-pass of the same side-looking satellite are required in order to detect the ground deformation (Modified from Chen, 2010).

Pair	Master	Slave	Baseline	Days
1	1/7/2007	1/12/2009	820m	736
2	2/22/2007	8/25/2007	817m	184
3	2/22/2007	8/30/2009	192m	920
4	8/25/2007	8/30/2009	699m	736
5	1/10/2008	5/27/2008	754m	138
6	2/25/2008	5/27/2008	229m	92
7	1/10/2008	2/25/2008	616m	46

Table 2.2: List of the seven interferograms generated. Older images are set as the reference image (Master image), while the younger images are set as slave images. Pair 3 was selected based on its low perpendicular baseline (< 500m) and the temporal difference (red boxes). On the other hand, pair 2 was selected based on its high perpendicular baseline.

recorded data is based on the size of the antenna or aperture. Larger antenna will result in higher spatial resolution. For SAR, a larger antenna is synthesized to improve the resolution, even though the antenna is smaller physically.

For InSAR, only the phase information is used. Included in the phase is the information regarding the distance between the satellite and the surface in the range direction (Figure 2.2). InSAR uses the phase difference between two SAR images over the same area to calculate the surface deformation. This technique is called Differential InSAR or D-InSAR. It has many variations depending on the number of repeat-pass SAR images used in the processing, such as 2-pass, 3-pass and 4-pass interferometry. The phase difference map is called an interferogram, which contains fringes with information regarding the deformation. However, there are many factors that contribute to the raw phase difference. This can be better understood from the formula below (Lubis et al.,2010):

$$\Delta\varphi = \varphi_{\text{topo}} + \varphi_{\text{orbit}} + \varphi_{\text{defo}} + \varphi_{\text{atmos}} + \varphi_{\text{noise}}$$

The phase difference has effects from the topography (φtopo), perpendicular baseline (φorbit), surface deformation (φdefo), atmospheric effects (φatmos) and phase noise (φnoise). Using interferometry software, the phase data that reflects the deformation can

be isolated from the noises. For instance, a DEM can be used to remove the topographic effects.

2.2.3 InSAR Processing

Two pairs of ALOS PALSAR images were processed using the ENVI Sarscape software (version 4.4) (Table 2.2). 3-pass D-InSAR technique was used to process the pairs. As the name implies, 3-pass interferometry requires three repeat-pass SAR images over the same region. In order to use 3-pass interferometry, two interferograms are needed. One interferogram will be used to detect the deformation, while the other will be used to create a topographic phase of the region. Pair 3 was used for deformation detection due to its low baseline (192 meters) and high temporal difference (920 days) (Table 2.2). In contrast, pair 2 was used to simulate the topographic phase due to its high baseline (817 meters) (Table 2.2). The topographic phase interferogram was used to remove the topographic noise and also the effect of the curvature of the earth. The processing steps to create the final displacement map are shown in Figure 2.3.

1) Co-registration of the SAR images pair

After the preliminary step of baseline estimation, co-registration of the selected image pair was done. Co-registration is an important first step, where the pixels for both images were sampled so that they correlated with each other. The pixels of the Slave image were shifted onto the corresponding pixels of the Master image in the range and azimuth directions. These shifts were calculated accurately using orbital information and the DEM.

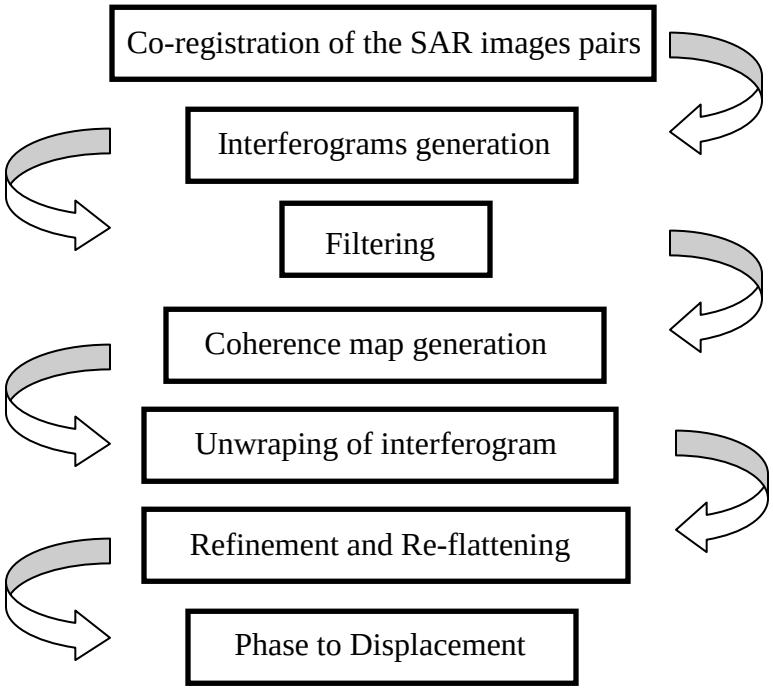

Figure 2.3: The InSAR processing steps taken to create the final displacement map.

2) Interferogram Generation

The next step is the generation of the interferograms and DEM flattening. By calculating the phase difference of the co-registered images, an interferogram was acquired. In this step, the topographic phase interferogram is essential in removing the topographic effect as well as the effect of the curvature of the earth due to the observation geometry.

3) Filtering

The Goldstein filter was used to filter the atmospheric noises and the phase noise (Goldstein and Werner, 1998). The phase noises are due to temporal and baseline decorrelation. The main purpose of the filtering step is to clarify the fringes and reduce noises without destroying valuable information (Utley, 2004). The details of the Goldstein filter algorithm can be found in a paper by Goldstein and Werner (1998).

4) Coherence Map Generation

After the interferogram was filtered, a coherence map was generated. A coherence map is used to detect the reliability and quality of the interferogram. The coherence map has a range of values from 0 (absolute noise) to 1 (absolute correlation).

5) Unwrapping of Interferogram

Unwrapping of the interferogram is the most complex step and it was done using the Growing Region algorithm (Reigber and Moreira, 1997). This is an important step to convert phase data, which is in terms of 2π, to absolute values. Other unwrapping algorithms include the branch-cut, minimum cost flow and minimum least squares.

6) Refinement and Re-Flattening

This step is basically recalculating the orbital information by selecting GCPs (Ground Control Points) on the interferogram. The GCPs were located on flat and high coherence areas (Sefercik et al., 2011).

7) Phase to Displacement

Finally, the absolute unwrapped phase data was converted to displacement. The final displacement map was geocoded.

2.3 2D-Seismic

2.3.1 Datasets and Processing

The seismic data were obtained from the Oil and Gas Development Company Limited Pakistan (OGDCL). These lines were processed and migrated by the company. The length of the profiles ranges from 7 to 40 km. The location of the lines is mostly in the Central Potwar Plateau region (Figure 2.4). Six selected seismic reflection profiles were interpreted for structural and stratigraphic information (Figure 2.5). Lines 782-CW-13, 782-CW-27 and 93-MN-09 are generally oriented north-south, while lines 782-CW-11, 782-CW-14 and 93-MN-10 are generally oriented east-west. These lines were selected as they were time migrated and had the least noise. The main focus of this study is to find as much about the Pre-Cambrian salt layer from the available seismic data. The software used for interpretation is SMT Kingdom, with the assistance of well data and published velocity model (Pennock, 1988; Chen, 2009). Seismic attributes, such as instantaneous phase, were used to easily detect horizons and faults. Finally, these interpretations were compared to published results from other parts of the SR-PP region.

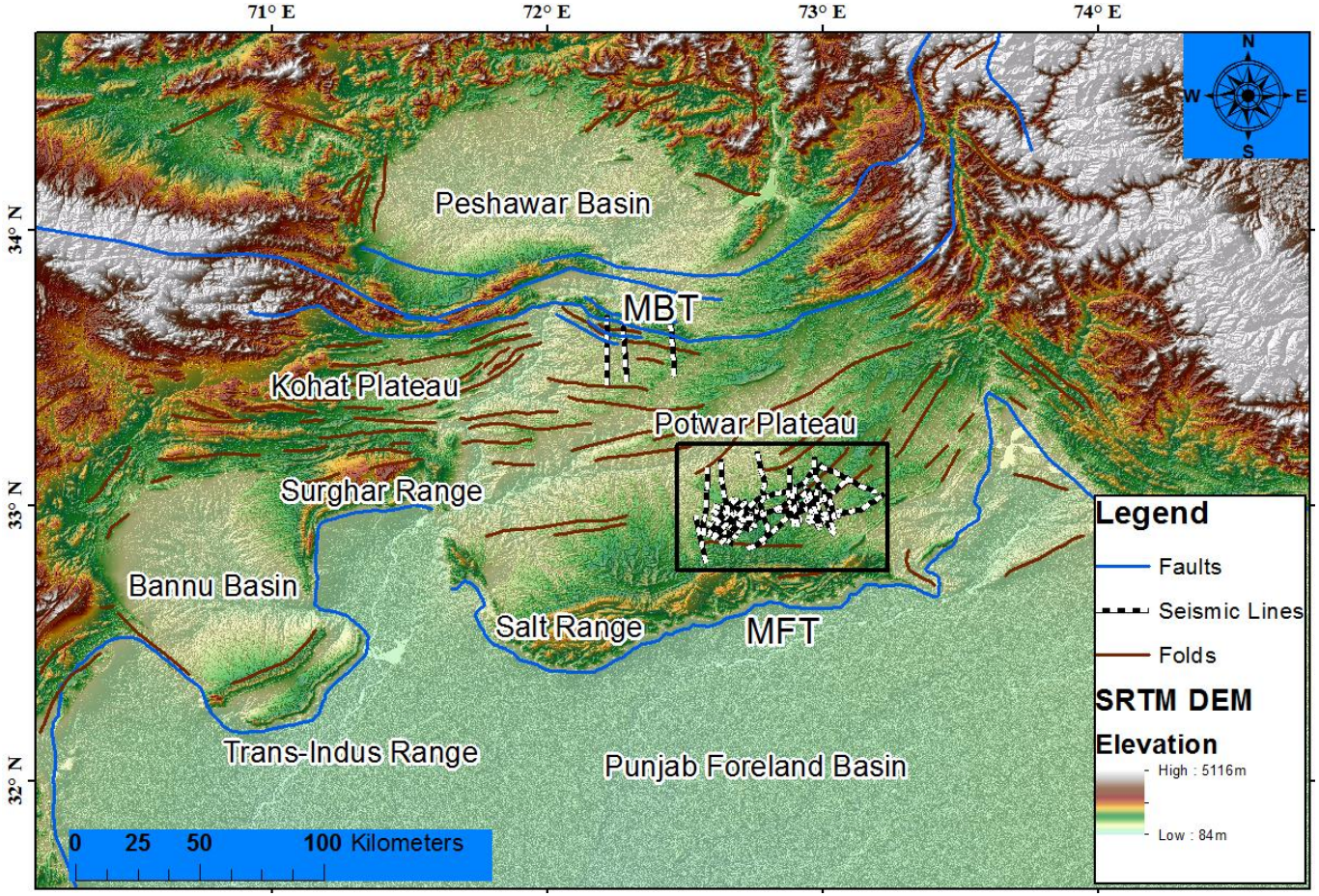

Figure 2.4: The black and white lines are the locations of the seismic lines. The lines are located to the east of the PALSAR scenes. The two main north dipping thrust fault systems in the area are the MBT (Main Boundary Thrust) and the MFT (Main Frontal Thrust). The background image is a 90m resolution SRTM DEM.

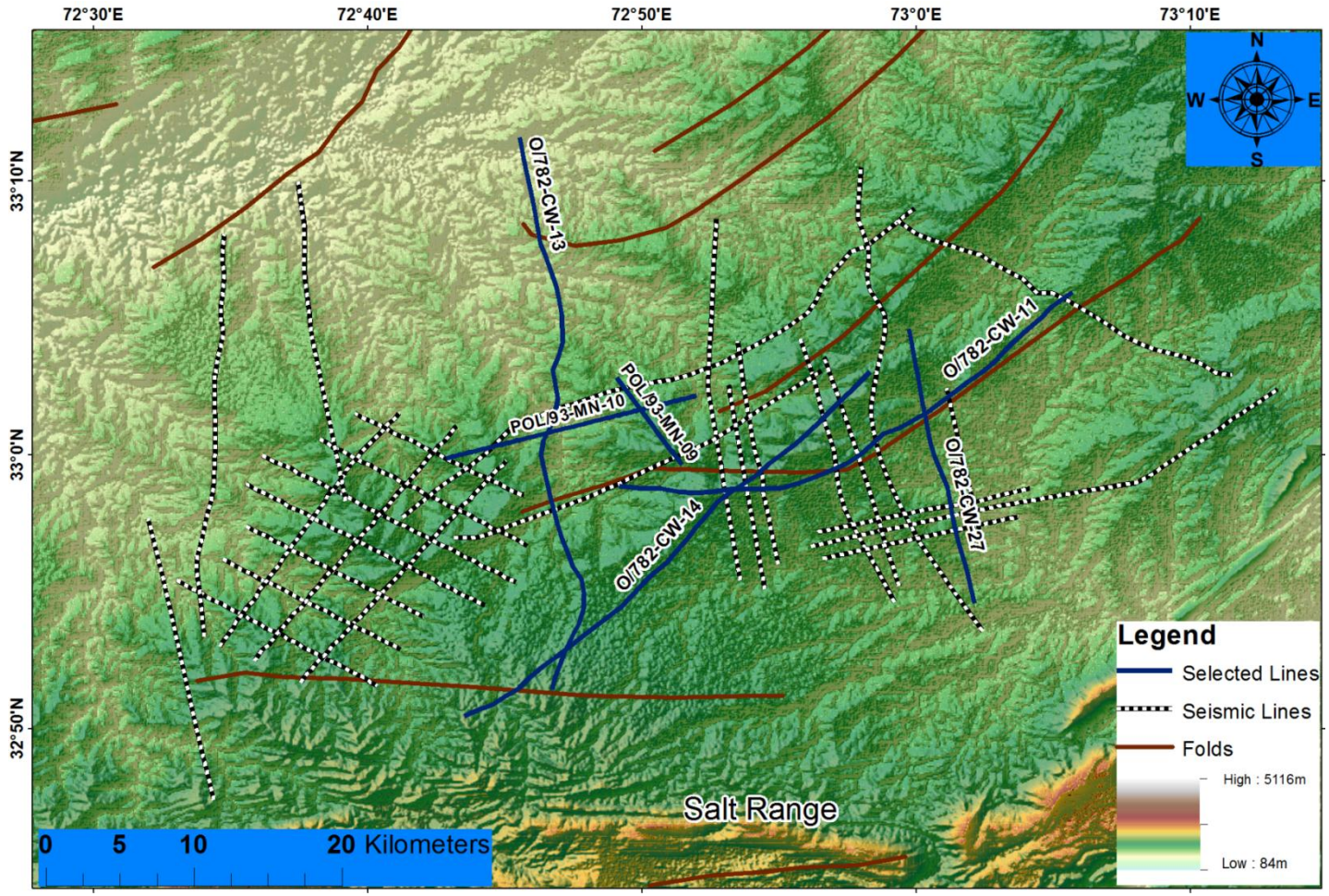

Figure 2.5: A topography map showing the interpreted seismic lines (navy blue lines).

The seismic lines were time migrated using finite difference time migration and filtered using F-X deconvolution method. Moreover, dynamite was used as the source for the surveys. Due to the complex subsurface structures in this region, the migration method is essential in order to interpret the subsurface accurately

Migration is a seismic processing technique that restores the seismic signals to their origin location. After migration, complex structures, such as salt domes, faults and folds, can be easily interpreted. There are two main types of migration, which are time migration (time domain) and depth migration (space domain). Depth migration is more accurate but requires more time and cost. Therefore, time migration is usually used for fast processing.

2.4 Mountain-front Sinuosity

2.4.1 Datasets and Processing

An Advanced Spaceborne Thermal Emission and Reflection Radiometer (ASTER) image was used to calculate the mountain-front sinuosity of the Salt Range region. Figure 2.6 shows the location of the ASTER image. Basically, the mountain-front sinuosity index shows the balance of a region between active tectonic forces that tends to produce straight mountain fronts and the strong forces of erosion that tends to cut into the fronts (Keller and Pinter, 2002). The following is the formula for mountain-front sinuosity:

$$S_{mf} = L_{mf}/L_s$$

Mountain-front sinuosity is the ratio between the length of the mountain front at the foot of the mountain (L_{mf}) and the straight-line length of the mountain front (L_s) (Keller and Pinter, 2002). High values of the index signifies that erosional forces are predominant, while low values (<1.4) signifies that the region is uplifting.

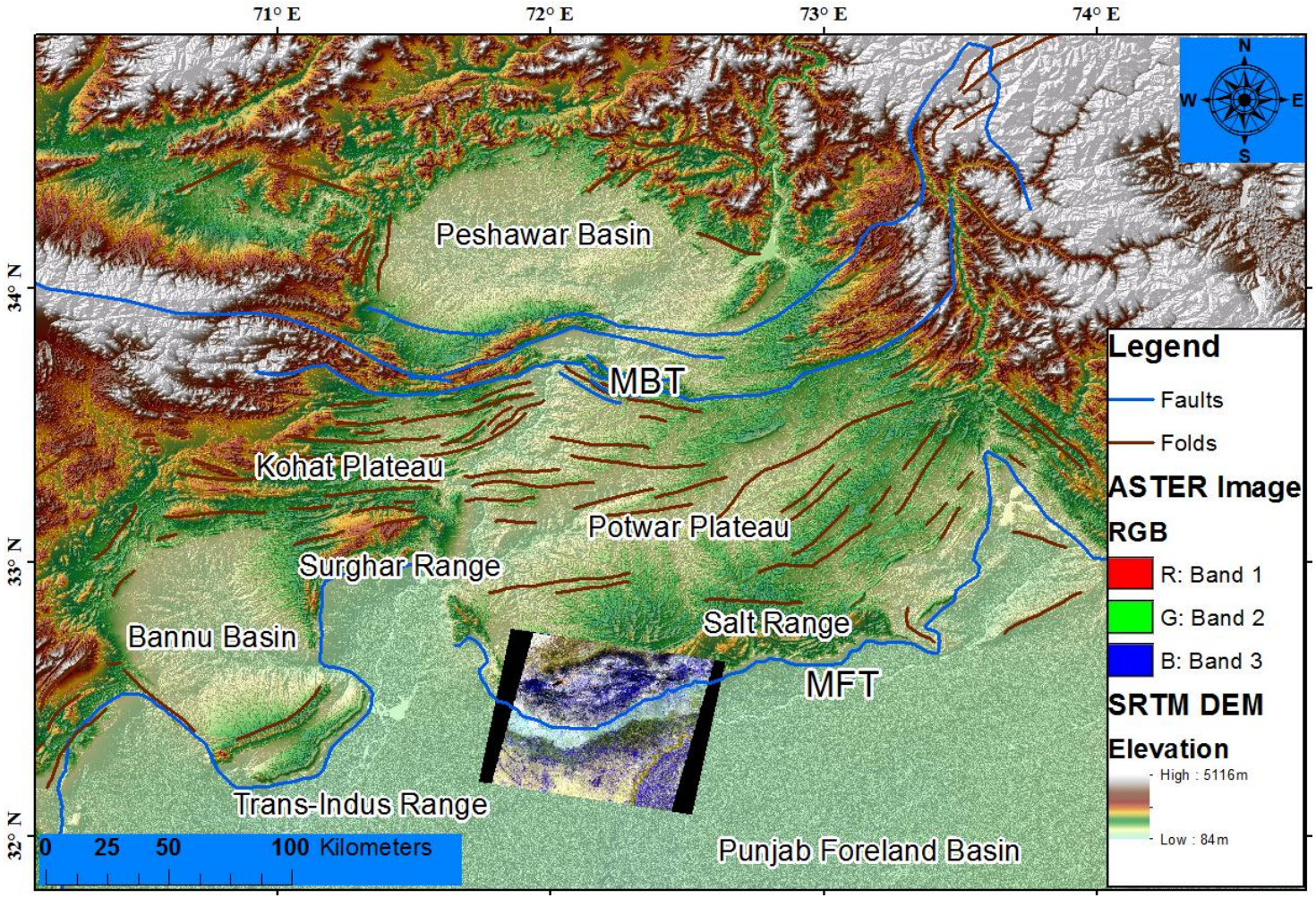

Figure 2.6: The location of the ASTER image used to calculate the mountain-front sinuosity. The image covers the western part of the Salt Range and part of the Punjab Foreland Basin.

Chapter 3:

Results

This chapter presents the results for the InSAR processing, 2-D seismic interpretations and mountain-front sinuosity calculations.

3.1 InSAR Results

3.1.1 Displacement Map

A displacement map was generated from stacking of two pairs of ALOS PALSAR images. The map presents the relative displacement for a time period in the LOS (Line of Sight) direction of the satellite. Basically, movements toward the satellite is regarded as surface uplift (blue and green colors), while movements away from the satellite is regarded as surface subsidence (hot colors). Figure 3.1 shows the relative displacement of the study region for the duration of approximately 2 years (February 22nd, 2007 to August 30th, 2009). Figure 3.1 will be referred to as DM1 (Displacement Map 1). In general, DM1 shows that the northern and the center parts of the Salt Range are uplifting. Although the displacement map shows displacement in the unit of mm/year, the result for the rate of uplift may not be reliable due to noises in the result. Also, there are displacement variations in the Potwar Plateau region. There are areas of the Salt Range that underwent subsidence, especially near the MFT. However, a majority of Salt Range is uplifted. This is consistent with other studies suggesting that the normal fault ramps that may be the cause of the uplift in the Salt Range region (Pennock, 1988; Jaume and Lillie, 1988). Furthermore, sharp changes in displacement can be observed at the northern and southern boundaries of the Salt Range. The southern boundary is most likely to be related to the Main Frontal Thrust (MFT).

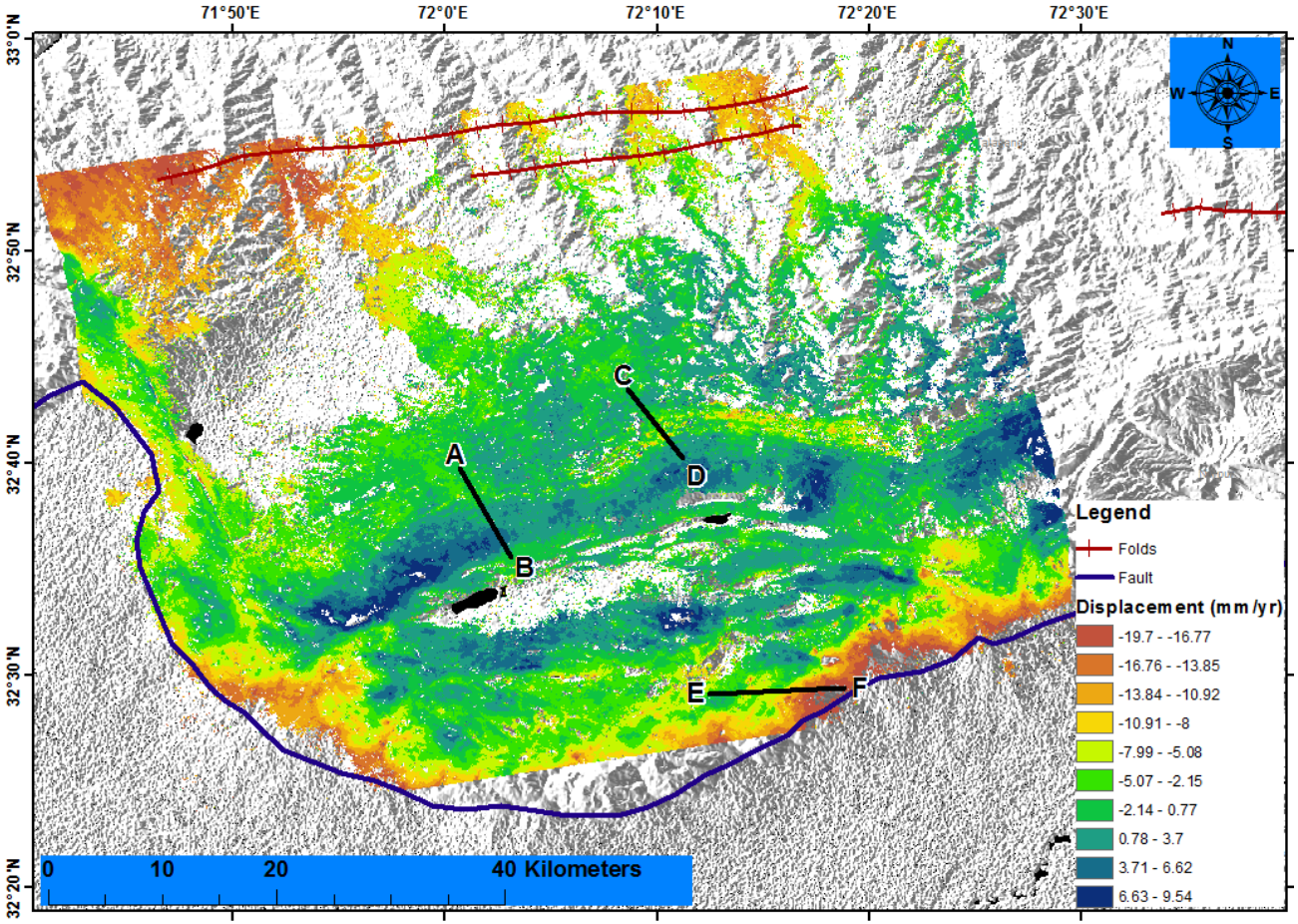

Figure 3.1: Displacement map in the LOS of western SR-PP region from February 22nd, 2007 to August 30th, 2009. Blue and green colors indicate movement towards the satellite (uplift). Orange and red colors indicate movement away from the satellite (subsidence).

Regions with no-data can be seen in DM1. These are areas with low coherence, where the phase data cannot reliably be converted into displacement (Figure 3.2). However, the map has more area with no-data in the northern part of the map. This is highly due to temporal decorrelation and vegetation growth as the time difference between the Master and Slave images is longer. Other areas with no-data are due to water bodies, such as Lake Uchalli (located at the center of Salt Range) and Lake Namal (located at the western boundary of Potwar Plateau).

In order to look at the displacement quantitatively, three (3) profiles of surface displacement were created for DM1 (Figure 3.3). All of the profiles show that the surface movement of Salt Range is mostly towards the satellite, which can be interpreted as uplifting. According to the profiles, the Salt Range is uplifting at a rate of approximately 2 mm/year. However, the profiles show that there is still residual topography in the displacement results. The effect of topography varies from profile to profile and this may be due to the inaccuracy of the DEM that was created (Figure 3.3). There are many differences between the profiles, which are explained below:

Profile A-B

Profile A-B runs across the northern boundary of the Salt Range. This is a good profile to calculate the uplift rate of the region because the northern boundary is related to the normal fault ramp. In contrast, the profiles across the southern boundary of the Salt Range are related to the MFT. Figure 3.3a shows that the displacement changes (A-B) from uplift to subsidence and finally uplift again.

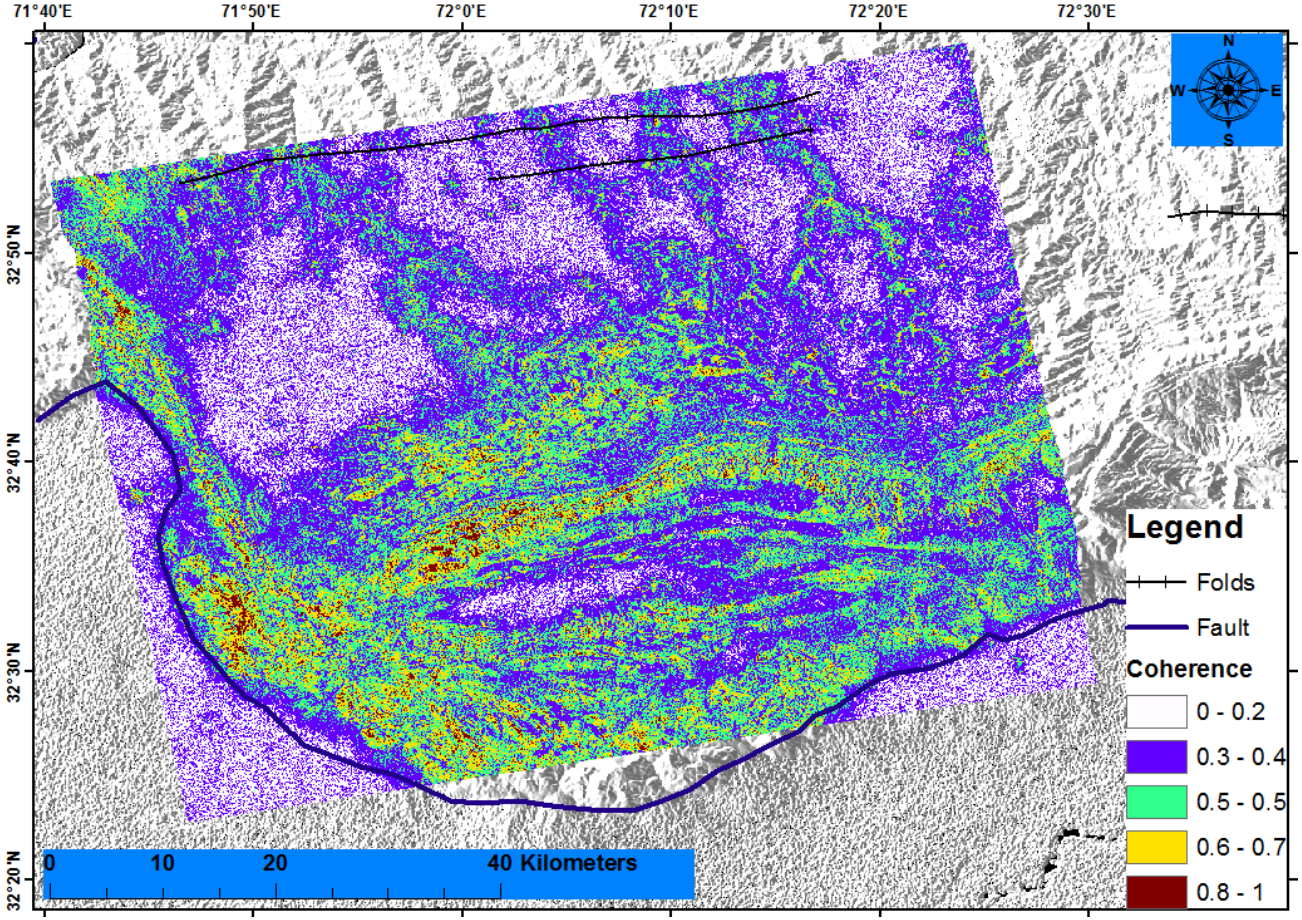

Figure 3.2: Coherence map for Displacement Map 1 (DM1). The measurement of coherence is a dimensionless unit from 1 to 0. Coherence of 1 means that there are no phase noise and the data is reliable, while 0 represents all noise and the data is unreliable.

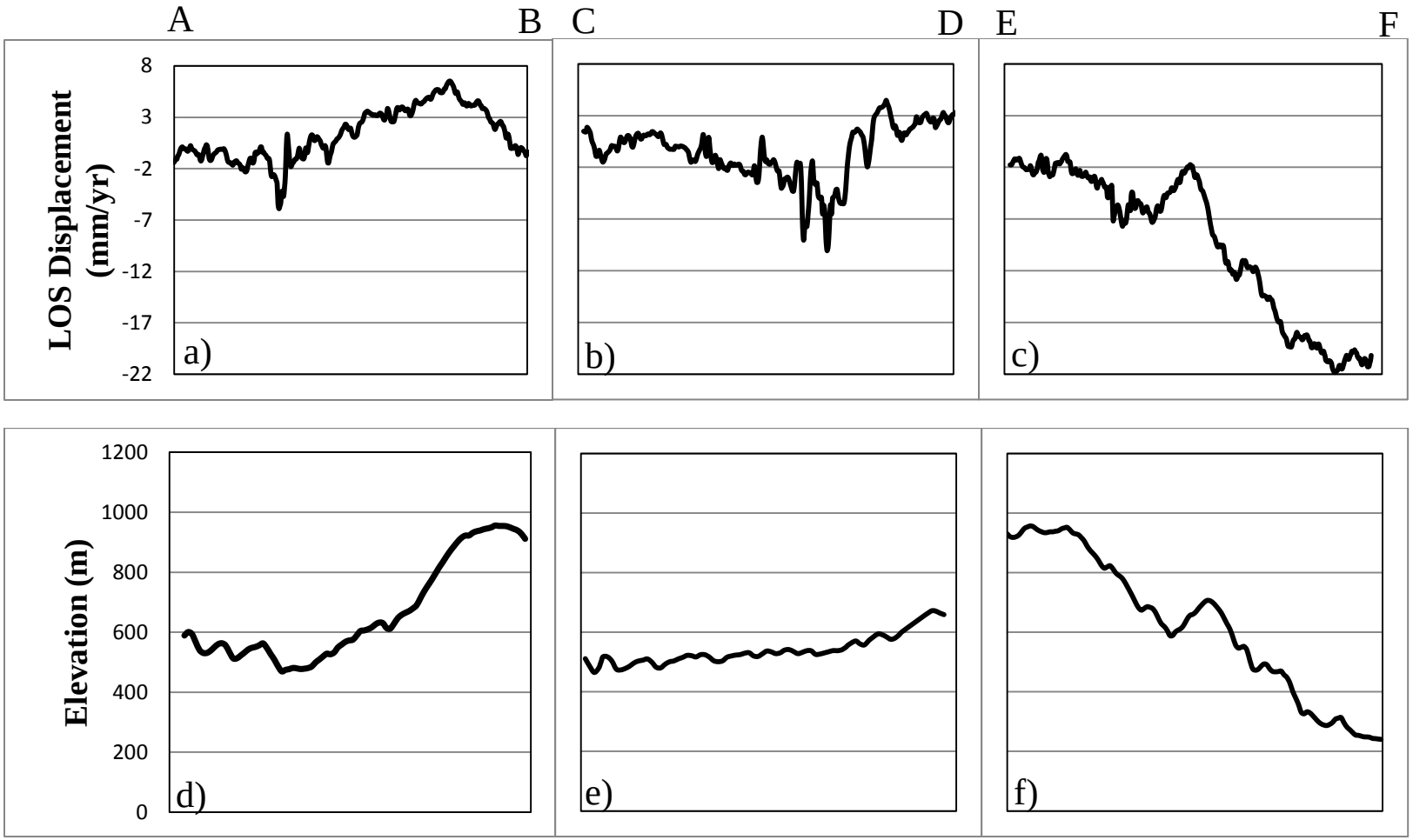

Figure 3.3: Profiles of surface displacement from Figures 3.2a-c, located along the cross-sections A-B, C-D and E-F respectively in the DM1. Figures 3.2 d-f are the corresponding topography for the three profiles.

Profile C-D and Profile E-F

Profile C-D is similar to profile A-B, but is located to the east of the profile. Profile C-D shows uplift in the Salt Range region. Compared to others, profile C-D has the least topography influence. On the other hand, profile E-F shows that the displacement follows the topography closely. Profile E-F displays the displacement profile of Salt Range to the west and the Punjab Plains to the east.

3.1.2 Coherence Maps

Coherence map of the interferogram shows the reliability and quality of the InSAR result. The measurements are dimensionless ranging from 0 to 1. Coherence data with a measurement of zero means that the phase information is all noise and will not be used to calculate displacement (Figure 3.2). On the other hand, coherence data with a measurement of 1 has no noise and is ideal for displacement calculation. Coherence is calculated by measuring the signal-to-noise ratio of each correlated pixel. The displacement map was generated using phase data with a coherence of 0.3 to 1. Furthermore, most of the high coherence areas are located at Salt Range, while areas of Potwar Plateau are of low coherence. These low coherence areas are mostly agriculture or highly vegetated land. Another pattern that is obvious is that most of the high coherence points are located in high terrain areas. These areas are mostly filled with ridges.

3.2 2D-Seismic

3.2.1 Interpretations

Six migrated seismic reflection profiles were interpreted using SMT Kingdom (Figure 3.4-3.9). These seismic profiles are commercial lines for oil and gas exploration in the South Potwar Plateau by OGDC. Well data and velocity models were used to interpret the profiles. Four main layers can be distinguished from each profile. They are, from the top, the molasse section (Siwalik and Rawalpindi from Pleistocene to Miocene), the carbonate platform (Eocene to Cambrian), the Pre-Cambrian Salt Range Formation (SRF) and the Pre-Cambrian basement. The most distinguishable layer in the sections is the carbonate platform. This layer is characterized by very strong reflectors that cut across the profile in a thin layer. Below the platform, the SRF is characterized by a seismically transparent layer. The boundary between the SRF and the basement rock is also a strong reflector, which is mainly due to the high acoustic impedence difference. The Siwalik and Rawalpindi groups are identified as moderate parallel reflectors. In all of the seismic profiles, the boundary between the Siwalik and the Rawalpindi is inferred. Generally, the carbonate platform thickness is consistent throughout all the profiles. The SRF has the most variation in thickness, which is due to its ductile nature. Following are the description of the interpreted seismic lines:

Line 93-MN-9 (Figure 3.4a-b)

Line 93-MN-9 shows highly deformed geological layers. A thrust fault cuts through from the Siwalik all the way to SRF. The displacement can be seen clearly from the carbonate platform. The thickness of the platform is consistent at around 600 meters.

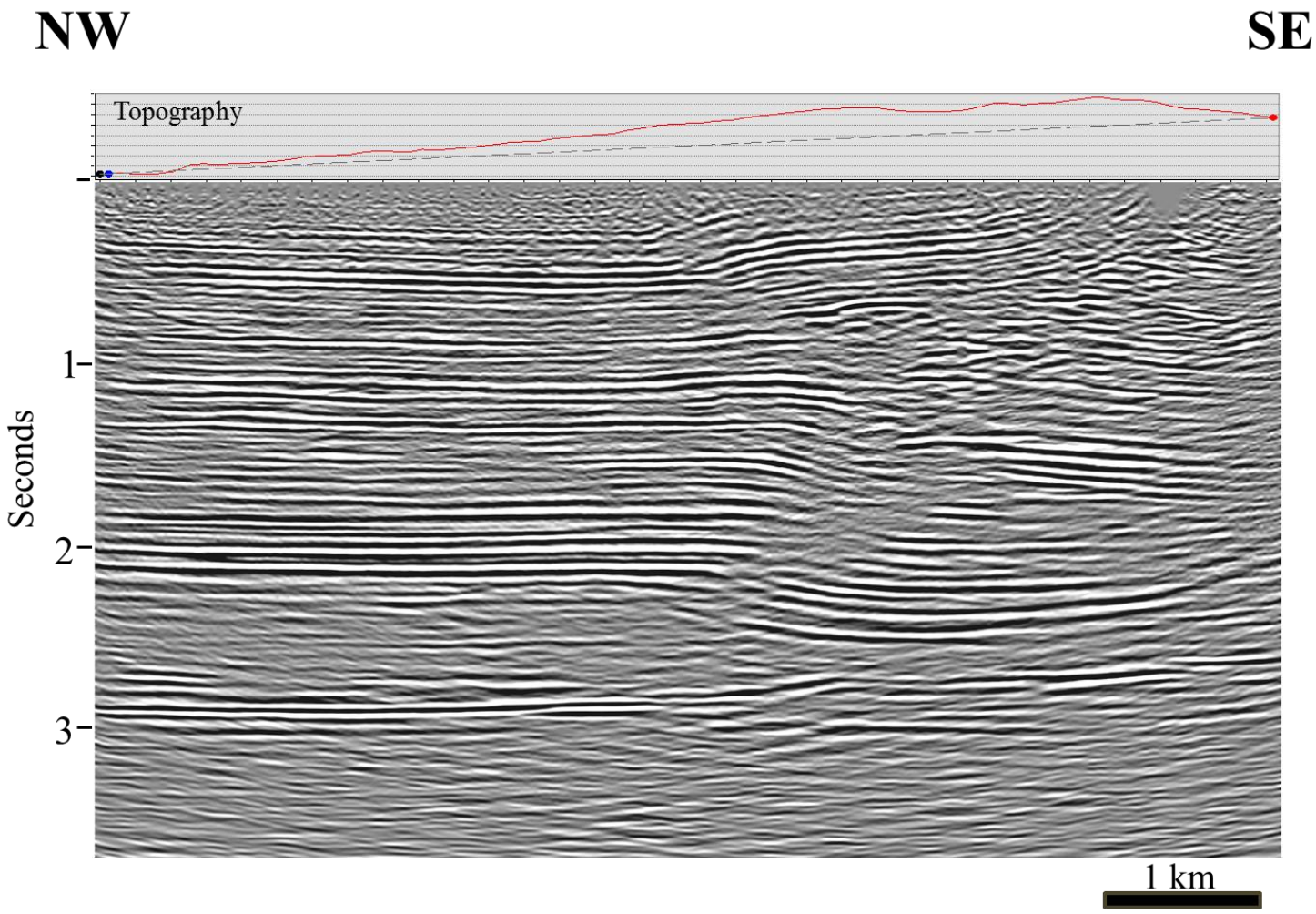

Figure 3.4a: Uninterpreted migrated seismic reflection profile Line 93-MN-9.

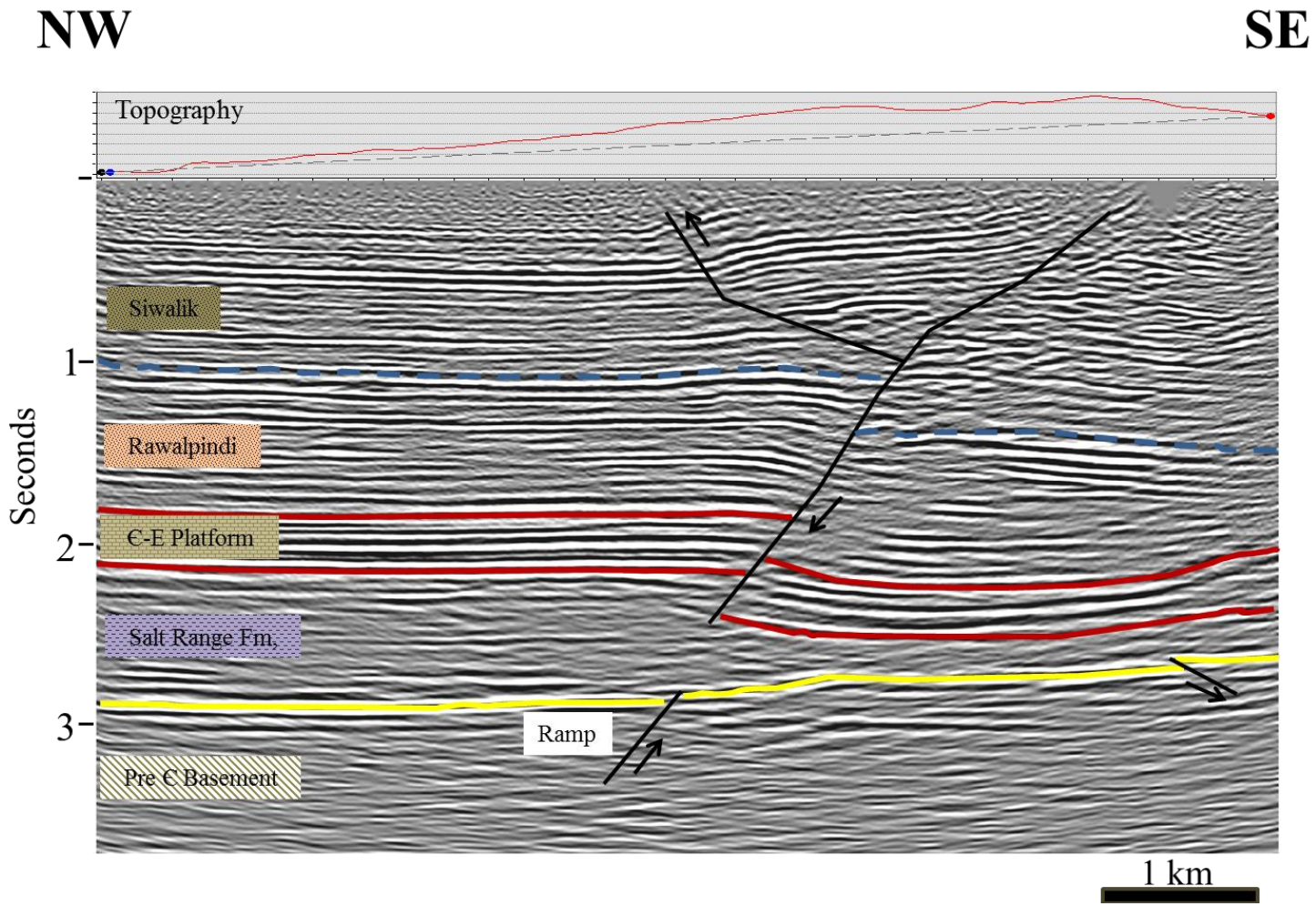

Figure 3.4b: Generalized interpretations of Line 93-MN-9. A large thrust fault cuts down the profile. The displacement can be seen clearly at the carbonate platform. A normal fault ramp is identified near the basement. Also, the different in the thickness of the salt layer can be attributed to the faulting in the profile.

Furthermore, the thickness of the SRF varies on both sides of the thrust fault. The salt is much thicker on the northwestern side (~1800 m) than the southeastern side of the profile (550-660 m). The thinning of the salt is due to the main thrust fault and a normal basement fault. Both of these faults compress the salt layer. The depth to the top of the salt (~3500 m) is more than the 1500 meters threshold, where the salt layer could overcome the strength of the overburden and move upwards. Moreover, the normal basement fault acts a ramp and causes the overburden to be uplifted. A small thrust fault also cuts the basement rock, which could also act as a ramp. Other structures that can be distinguished are another thrust fault branches off the main fault resulting in a pop-up structure. Finally, the basement is dipping to the south at a dip of around 3.7 degrees.

Line 93-MN-10 (Figure 3.5a-b)

Line 93-MN-10 is generally oriented east-west. This profile is very different from Line 93-MN-9 as there is very little deformation of the layers. By comparing both lines, we can see that most of the deformation is due to compressional forces that are oriented north-south. All of the layers are relatively flat across the profile. The thickness of the platform is approximately 500 meters. The thickness of the salt layer is constant at around 1800 meters. The artifact located in the basement rock could be due to error in processing, such as migration.

Line 782-CW-11 (Figure 3.6a-b)

Line 782-CW-11 shows highly deformed layers in the SR-PP region, with the layers are gently folded. A thrust fault can be seen cutting the carbonate platform with the hanging wall on the northeastern side and the foot wall on the southwestern side.

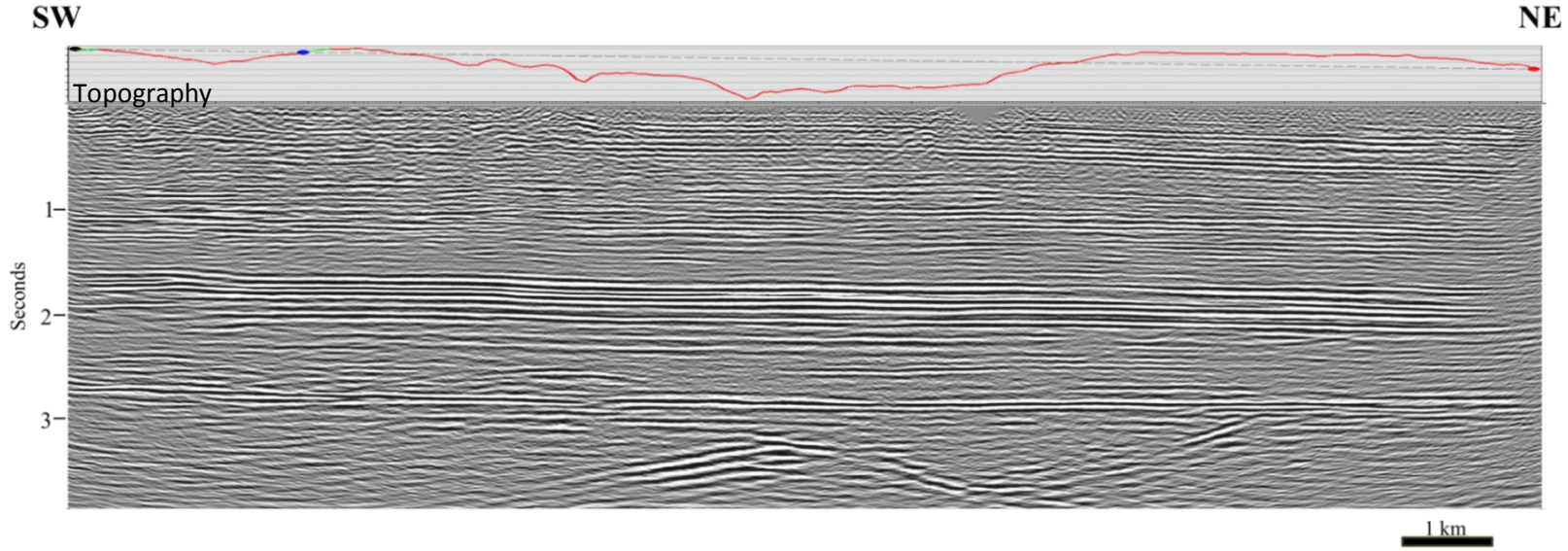

Figure 3.5a: Uninterpreted migrated seismic reflection profile Line 93-MN-10.

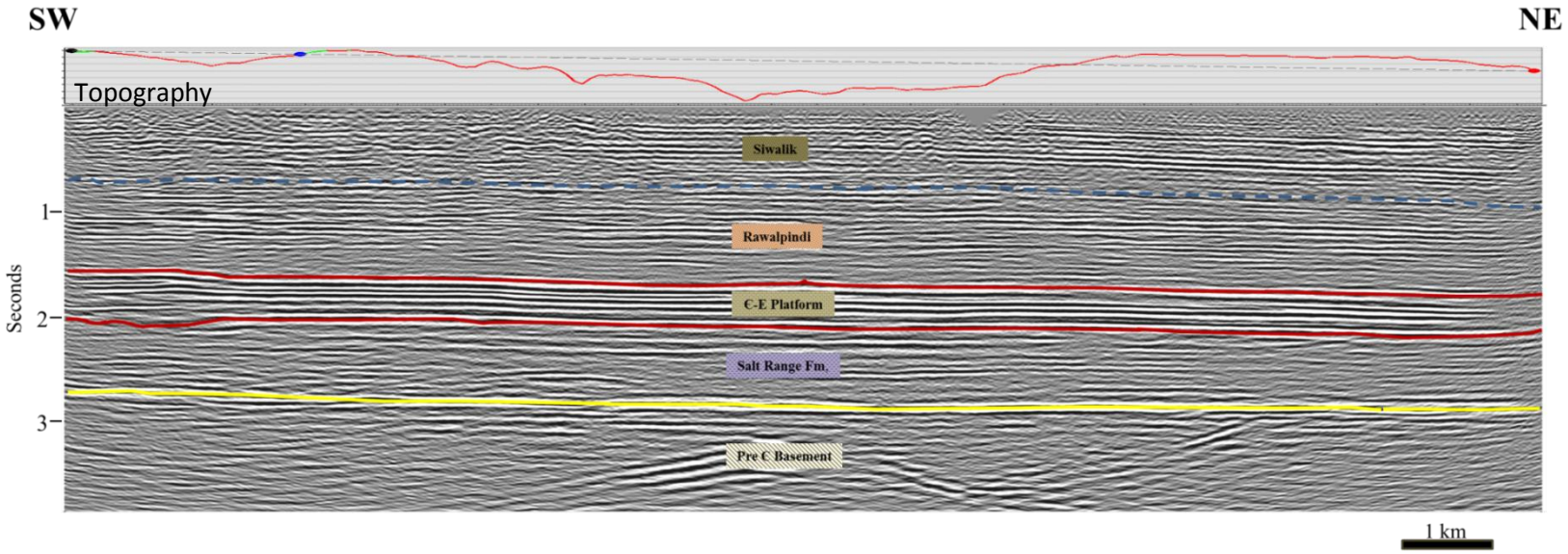

Figure 3.5b: Generalized interpretations of Line 93-MN-10. Most of the layers are undeformed, when compared to Line 93-MN-10. The reflectors below the basement may be due to artifacts during processing.

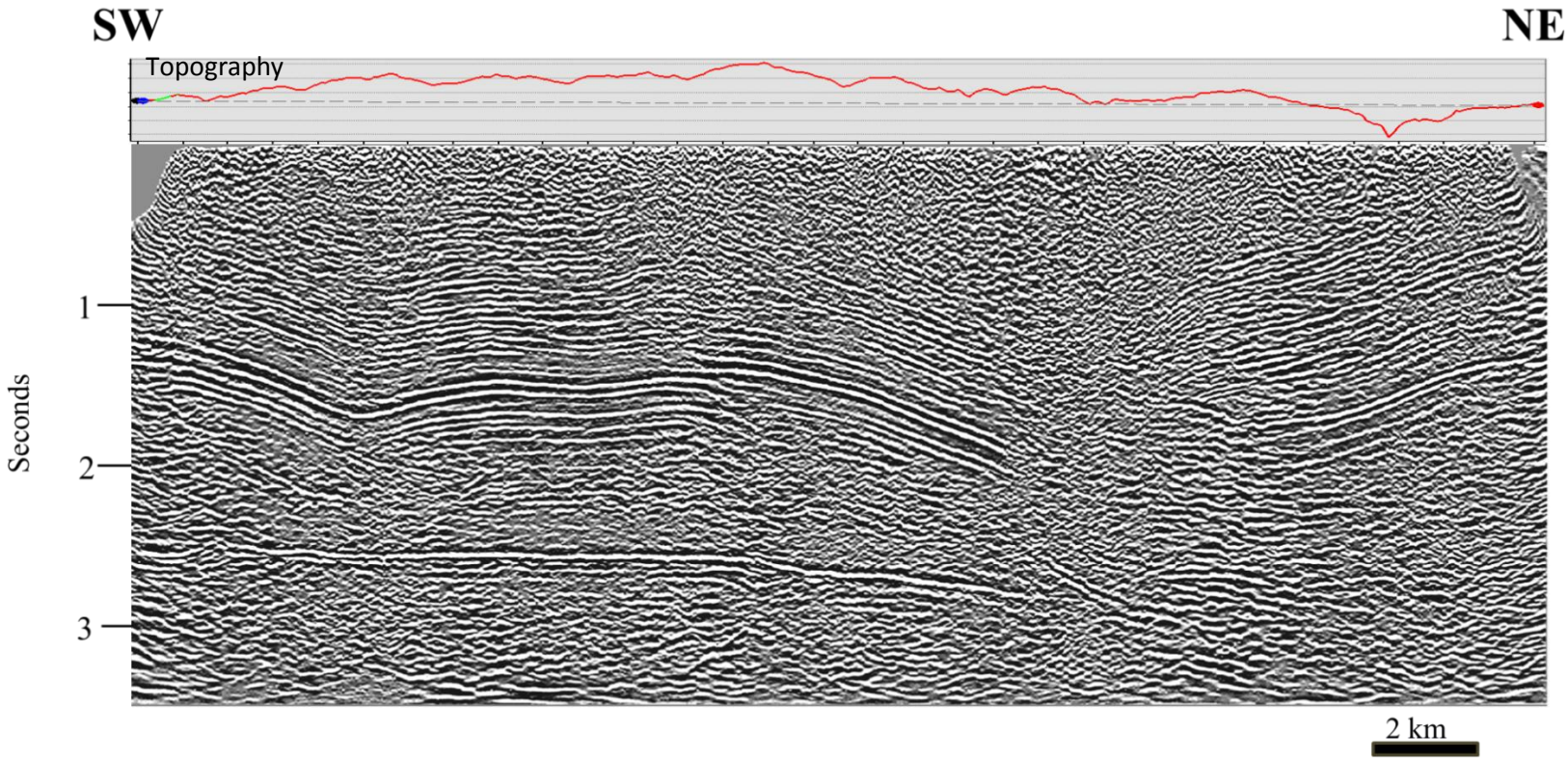

Figure 3.6a: Uninterpreted migrated seismic reflection profile Line 782-CW-11.

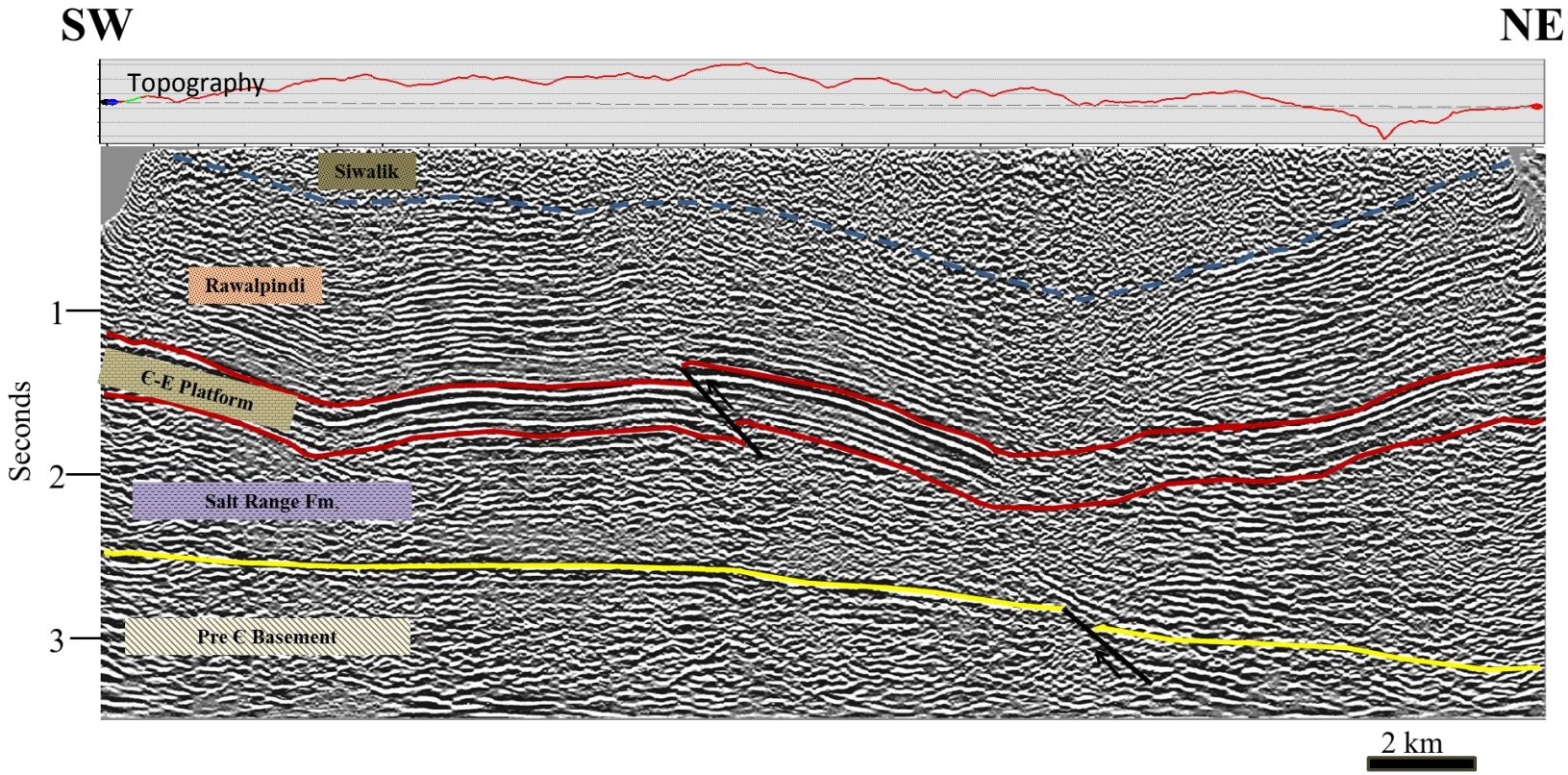

Figure 3.6b: Generalized interpretations of Line 782-CW-11. A normal fault ramp is identified ramping to the south. A syncline is located above the ramp. Furthermore, the variation in salt thickness can be attributed to folding of the layers.

Similar with other profiles, the carbonate platform (~600 m) is characterized by strong reflectors and can be easily distinguished. The salt thickness varies from 1100 meters to 5300 meters. Furthermore, a normal fault ramp at the basement can be seen clearly in the profile. Above the normal ramp is a section of very noisy seismic signals, which is interpreted as a syncline. This could also be due to error in migrating the seismic section.

Line 782-CW-13 (Figure 3.7a-b)

Line 782-CW-13 is the longest seismic profile interpreted and it shows gentle folding concentrated above the normal fault ramp. This structure is similar to the ramp from the previous line, where it is ramping towards the south. Moreover, the salt layer greatly varies in thickness from 440 meters to around 1800 meters.

Line 782-CW-14 (Figure 3.8a-b)

The structure in this line is similar to those interpreted in line 93-MN-9. A thrust fault through the carbonate platform is located above a normal fault ramp. Again, the salt layer varies in thickness (440 m to 2100 m), while the platform has a relatively constant thickness of 600 meters. The molasses and the carbonate platform displays gentle folding.

Line 782-CW-27 (Figure 3.9a-b)

Line 782-CW-27 is oriented north-south. A normal fault ramp is interpreted with a syncline located above it. Furthermore, the layers above the SRF are highly folded. The thickness of the carbonate platform (600 m) is consistent with other seismic profiles, while the salt layer has thickness that varies from 900 meters to 2000 meters. Similar to other lines, the seismic signals above the ramp is very noisy.

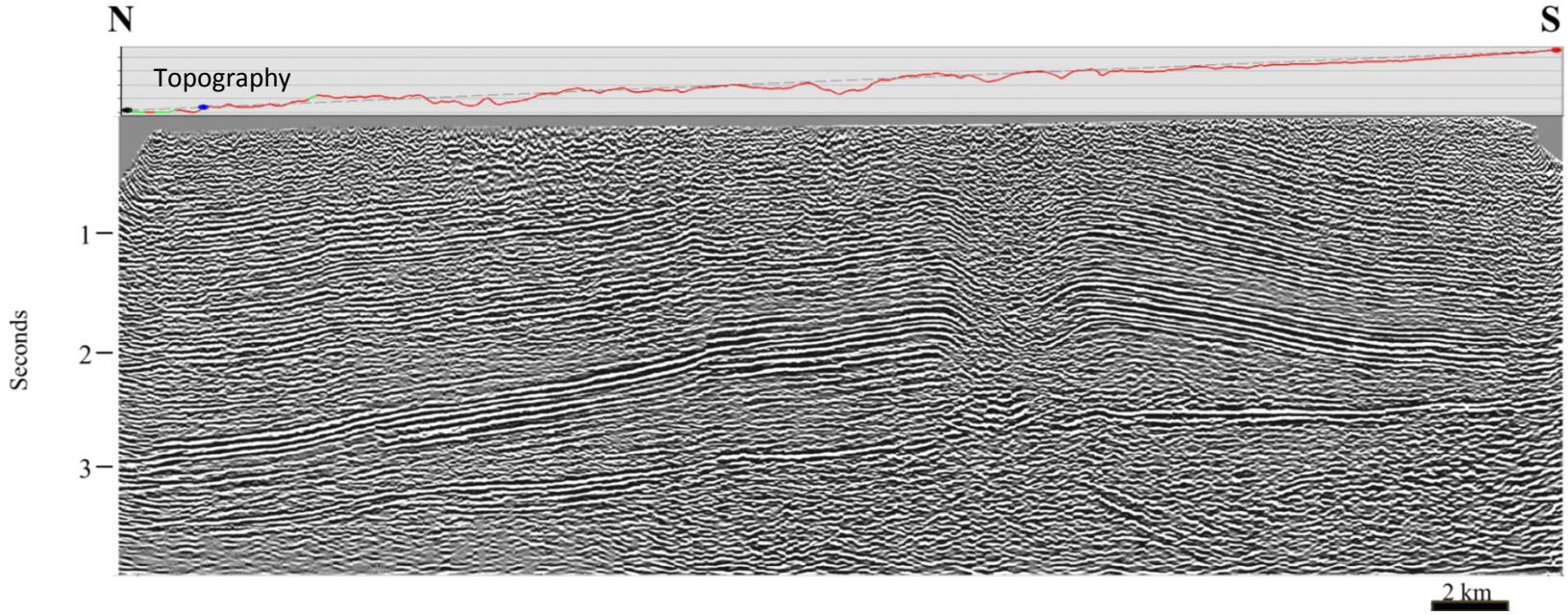

Figure 3.7a: Uninterpreted migrated seismic reflection profile Line 782-CW-13.

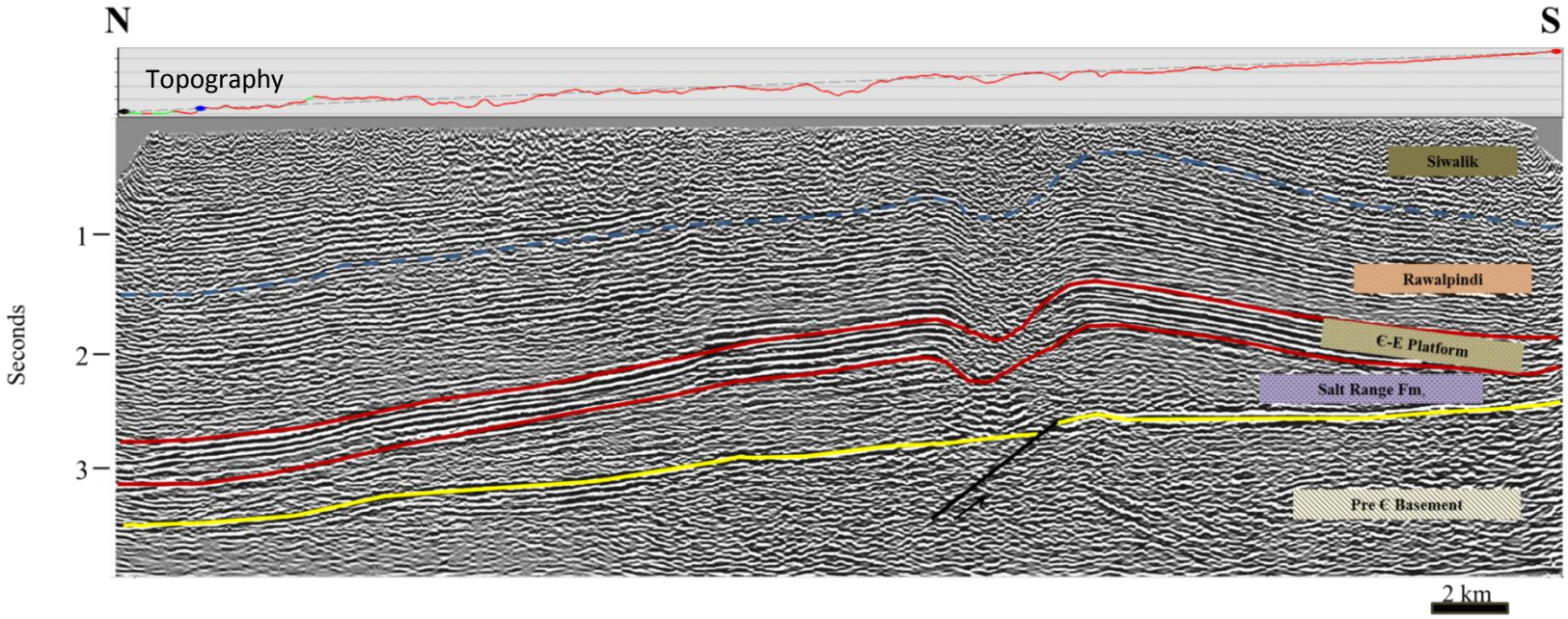

Figure 3.7b: Generalized interpretations of Line 782-CW-13. This profile shows a clear image of the normal basement fault ramping to the south. Similar to Line 782-CW-11, a syncline is located above the ramp.

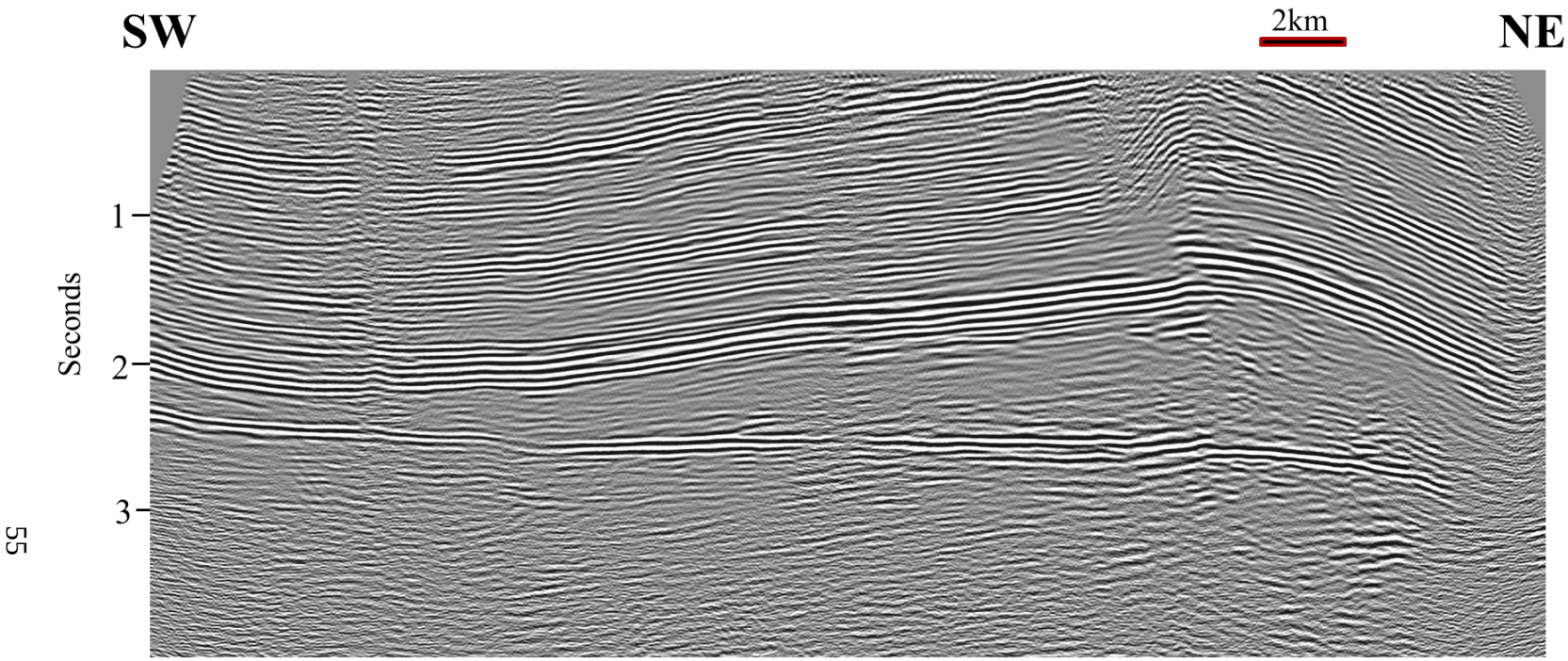

Figure 3.8a: Uninterpreted migrated seismic reflection profile Line 782-CW-14.

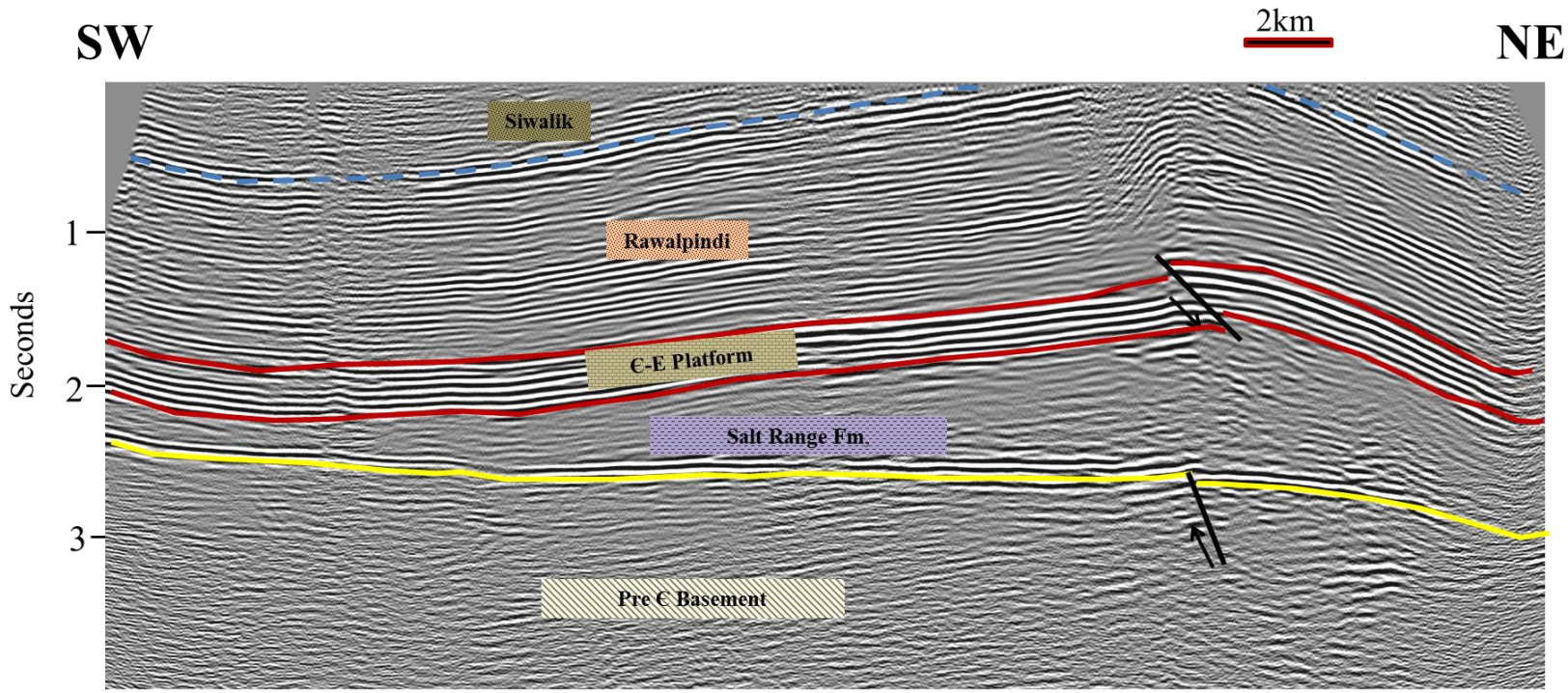

Figure 3.8b: Generalized interpretations of Line 782-CW-14. The structures displays gentle folding. A normal basement fault ramp and a thrust fault are identified.

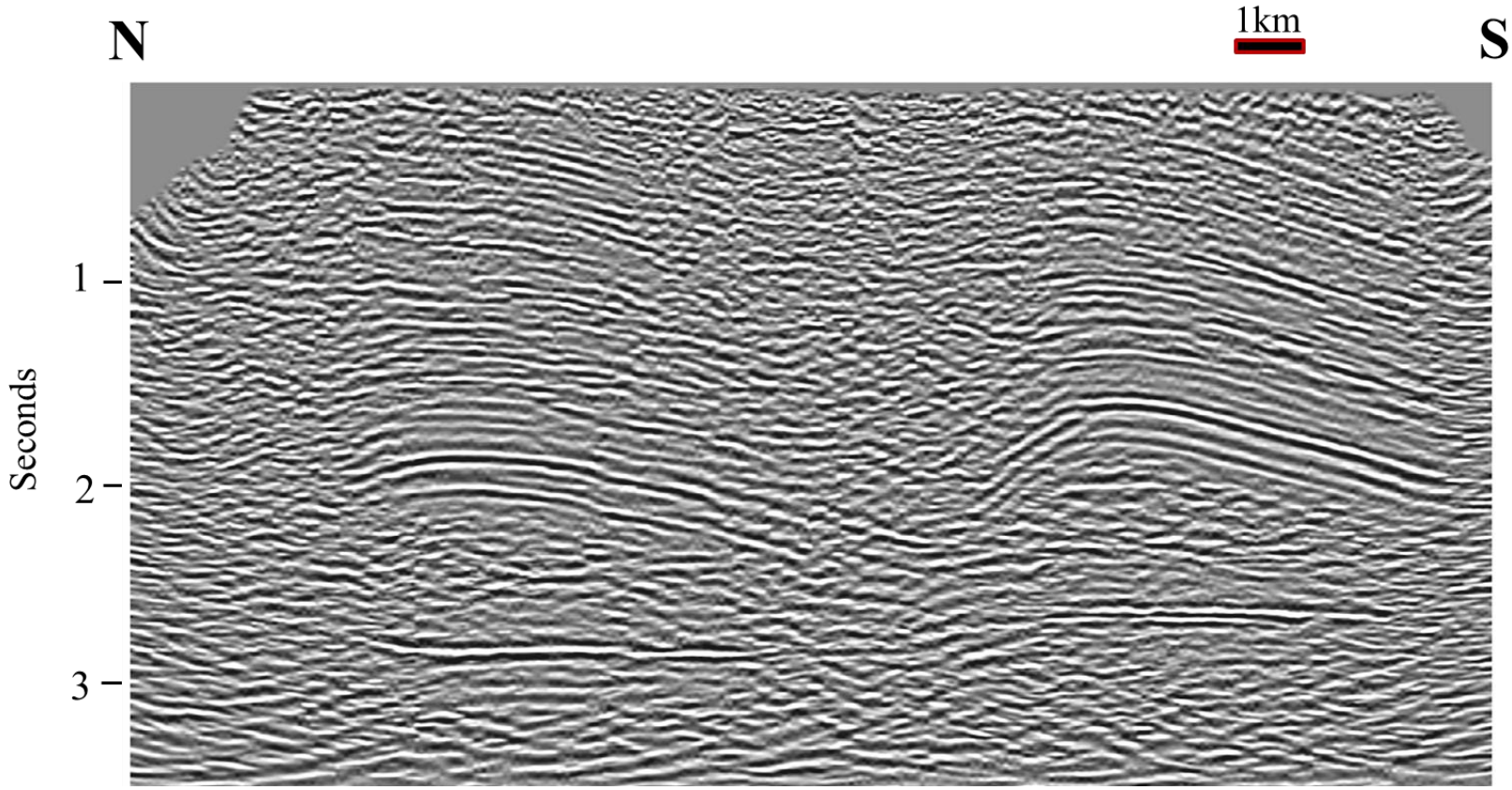

Figure 3.9a: Uninterpreted migrated seismic reflection profile Line 782-CW-27.

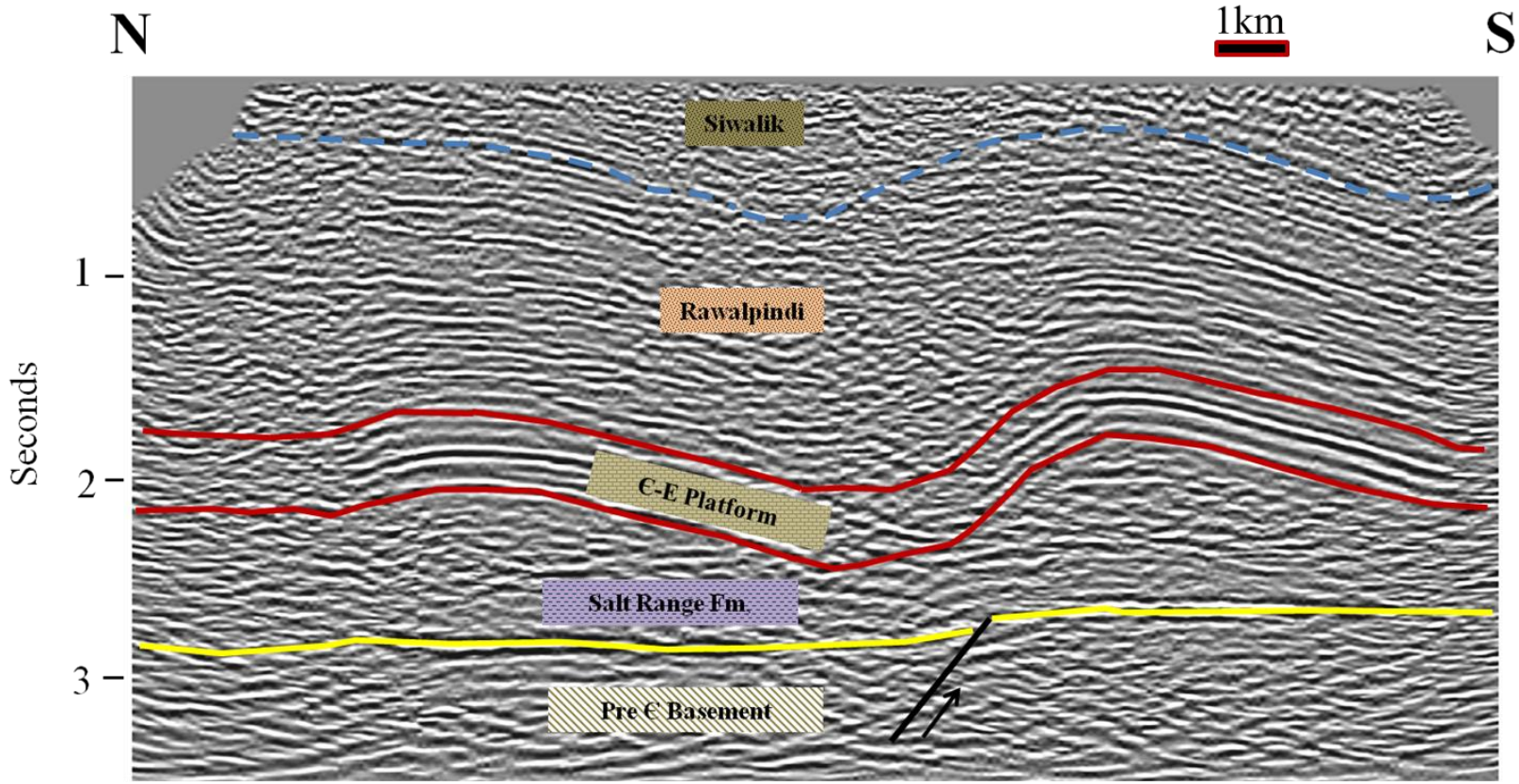

Figure 3.9b: Generalized interpretations of Line 782-CW-27. This profile shows a similar association between normal fault ramps and highly folded structures.

3.3 Mountain-front Sinuosity

3.3.1 Index Calculations

Two areas (Area 1 and Area 2) near the northern boundary of the Salt Range were chosen, in order to calculate the mountain-front sinuosity index (Figure 3.10). According to a study by Bull and McFadden (1977), a mountain-front sinuosity index of around 1 to 1.6 reflects active tectonics, which may suggest uplift in the Salt Range region. Area 1 has an index of approximately 1.25 and Area 2 has an index of approximately 1.03 (Figure 3.11 and Figure 3.12). These calculations suggest that the area may be undergoing uplift. It must be stressed that this method is only an approximate and shows relative balance between the tectonic forces and the erosional forces that influence this region.

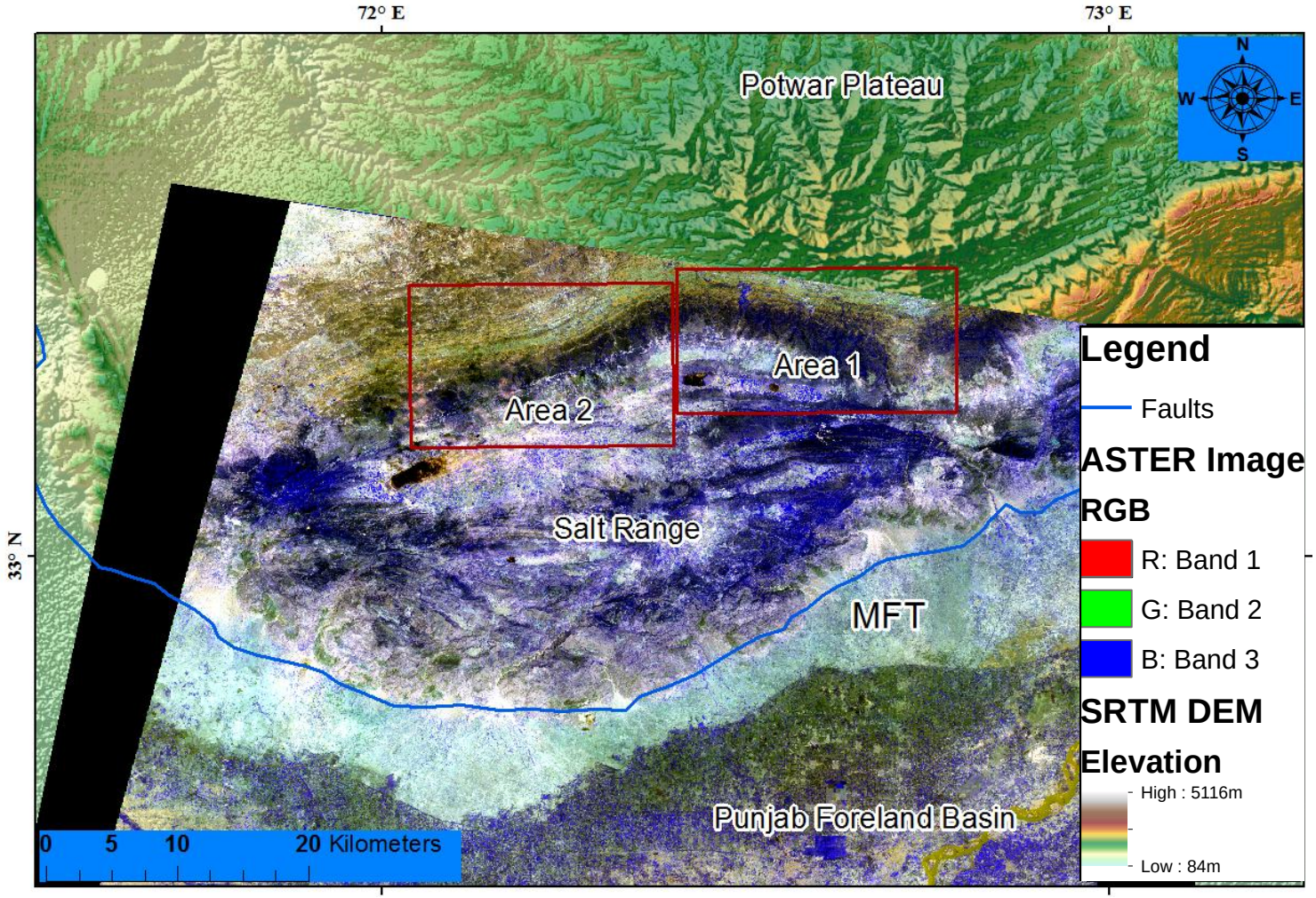

Figure 3.10: This map shows the location of the ASTER image, as well as the locations of Area 1 and Area 2. Both areas are located at the northern boundary of the Salt Range.

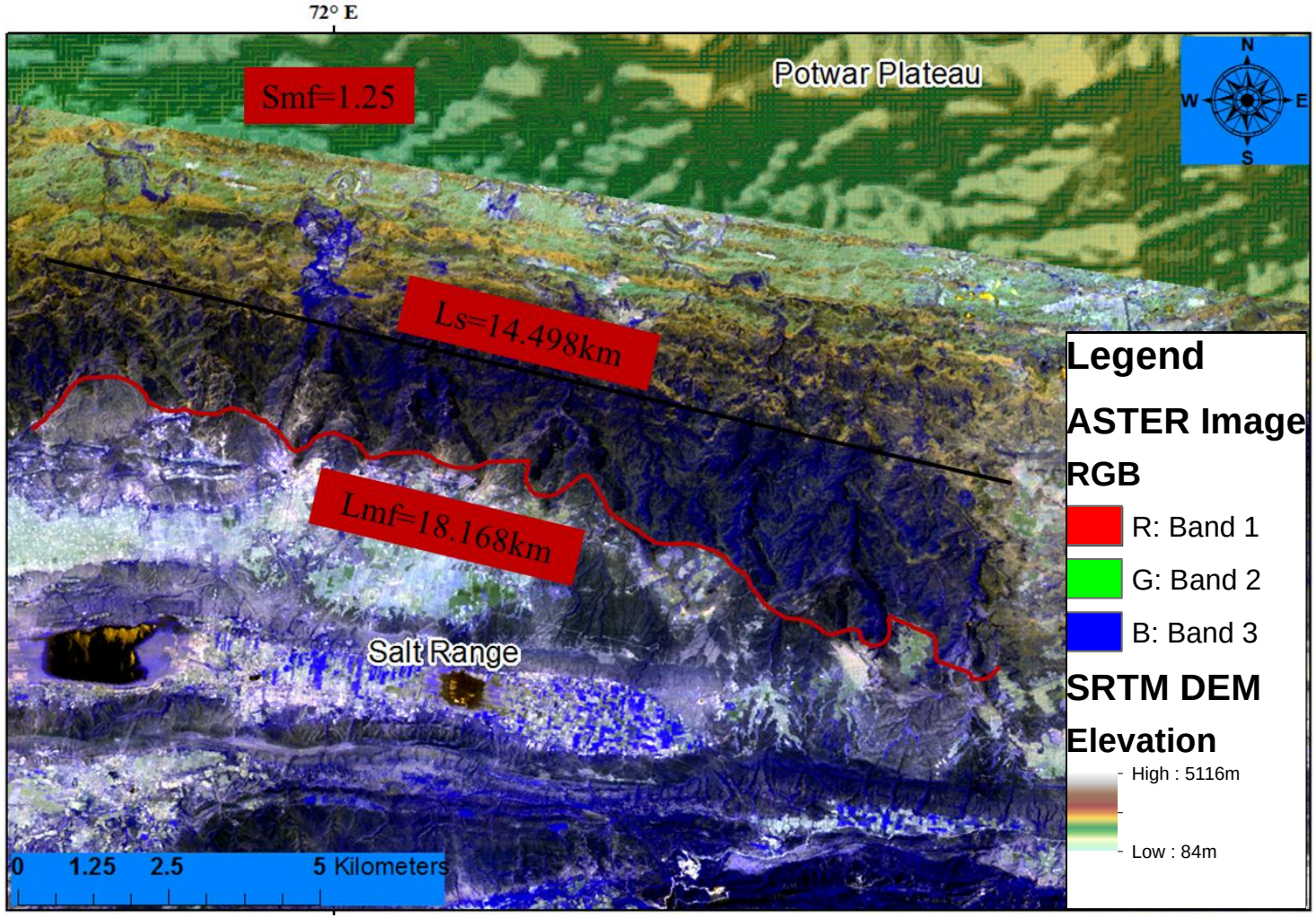

Figure 3.11: A map of Area 1. The RGB combination of this ASTER image is 123. The mountain-front sinuosity index is approximately 1.25 for this area, which suggests that the Salt Range may be undergoing uplift.

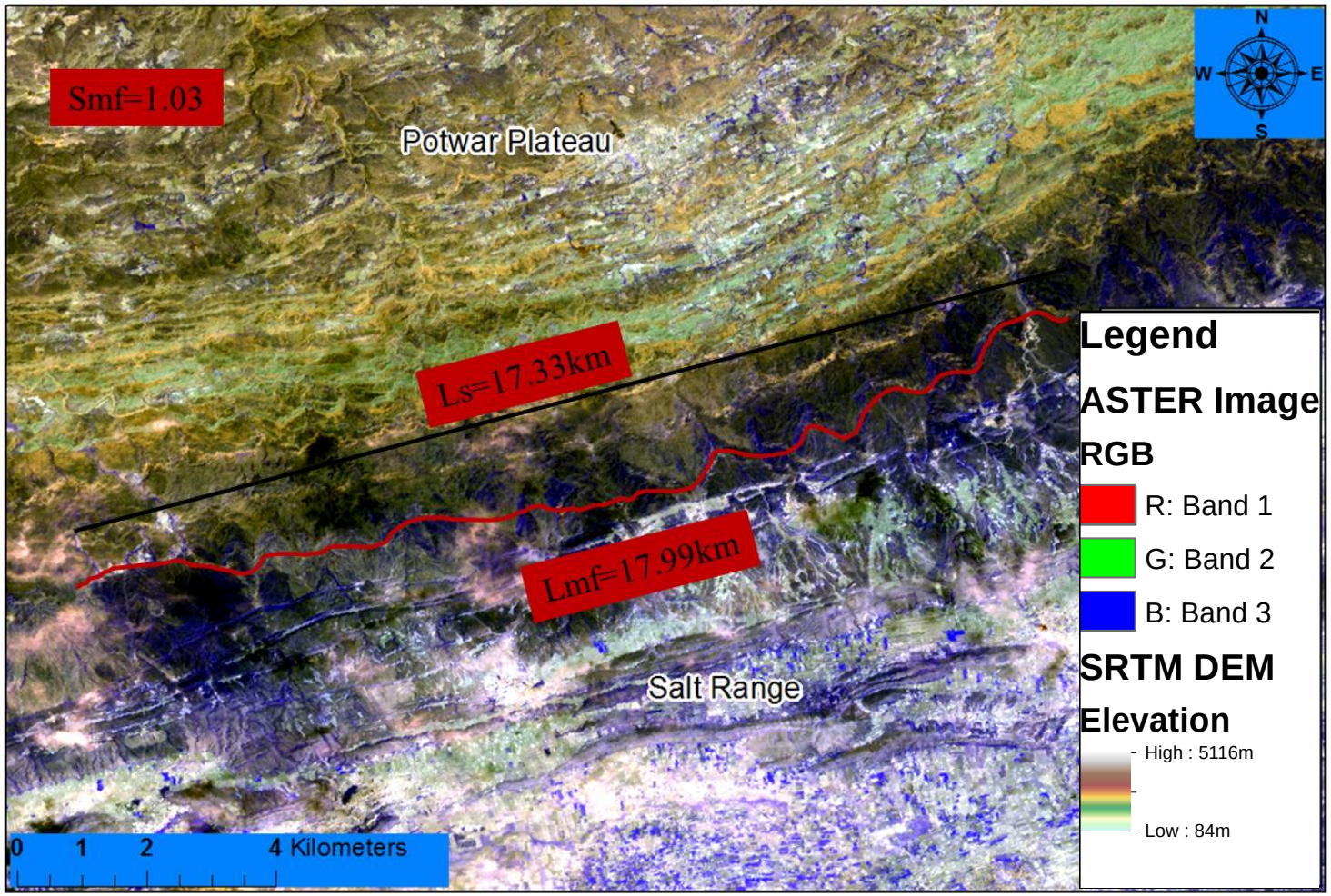

Figure 3.12: A map of Area 2. The RGB combination of this ASTER image is 123. The mountain-front sinuosity index is approximately 1.03 for this area, which suggest that the Salt Range may be undergoing uplift.

Chapter 4:

Discussions and Conclusions

This chapter discusses the implications of the InSAR result and seismic interpretations of the Salt Range and Potwar Plateau region. From the InSAR result, we can compare the movement of the Potwar Plateau and the adjacent Kohat Plateau. Moreover, seismic interpretations show the different geological structures that can affect the deformation in the region. The thickness as well as the depth to the salt was calculated using the seismic data. Furthermore, evidence of normal ramps in the seismic observations suggests that they could be the cause for the uplift seen in the InSAR results. The mountain-front sinuosity index calculations suggest that the northern part of the Salt Range may be undergoing uplift. Also, potential hydrocarbon traps are explained in this chapter. Finally, the roles of salt as a decollement or salt flow are discussed.

4.1 Discussions

4.1.1 Surface Deformation of Salt Range-Potwar Plateau Region

Interferometric Synthetic Aperture Radar techniques were used to detect the surface displacement of the western Salt Range-Potwar Plateau region. Chapter 3 displays the 3-pass InSAR result in a displacement map (DM1) of about 2 years temporal difference. L-band images from ALOS PALSAR were used in the InSAR processing. Result from a GPS stations was compared to the InSAR results by converting the LOS displacements into horizontal displacements (Khan et al., 2008). The InSAR result shows that the surface is mainly displaced eastward. This is similar to the GPS results that show the movement to the southeast in reference to India (Khan et al., 2008). However, there are limitations to the InSAR result, mainly due to topographic and atmospheric noises.

Atmospheric noises are random and can be effectively removed using an InSAR stacking technique, such as Persistent Scatterers. This technique requires a large number of images, which were not available for the study area. Therefore, 3-pass interferometry was chosen instead.

Previous InSAR studies have also been done in the Sub-Himalaya region of Northern Pakistan, notably in the Kohat Plateau (Satyabala et al., 2012) and the Kalabagh fault (Chen et al., 2010). These studies were done to understand the movement of the plateaus and the mechanism that controls them. Results of this thesis support the existence of the salt layer as the main factor in deformation as well as dictating the movement of the overburden in the region. Basically, the salt layer in this region affects the advance of both the Potwar Plateau as well as the Kohat Plateau. It is suggested that the Potwar Plateau advanced more to the south due to a Pre-Cambrian salt layer acting as a decollement (Cotton and Koyi, 2000; Jaume and Lillie, 1988). This is evident in the fact that the Kohat Plateau has more internal deformation than the Potwar Plateau. The key is the friction between the overburden and the basement rock. In the Potwar Plateau, the salt layer acts as a lubricant and decreased the friction significantly. This is supported by more internal deformation in the Kohat Plateau than the Potwar Plateau. This model is called the bulldozer wedge model, where the Potwar Plateau is suggested as a wedge that is moving on a ductile substrate (Cotton and Koyi, 2000; Lillie et al., 1987) (Figure 4.1). The wedge is essential for the generation of a thin-skinned fold-and-thrust belt, such as the SR-PP (Chapple, 1978; Davis et al., 1983). The wedge is thickest at the back part near the thrust and thins out in the direction of the thrust.

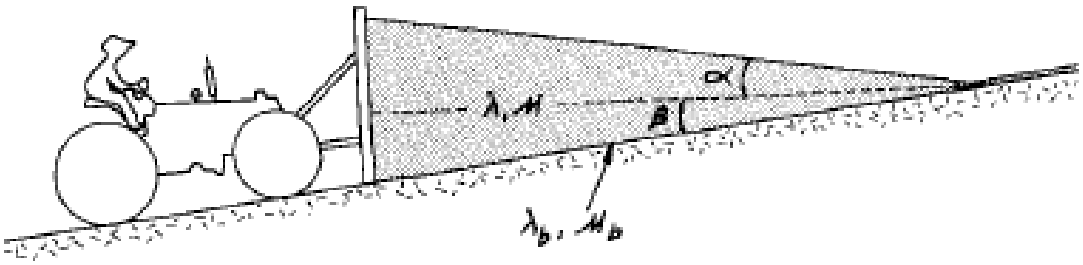

Figure 4.1: A bulldozer wedge model (Lillie et al., 1987). The taper angle is consists of the topography angle (α) and the basal angle (β). Increasing friction between the wedge and the basement will increase the taper angle.

Most of the deformation occurs near the back of the wedge and the thickness increases until an equilibrium state is achieved. Once equilibrium is achieved, the wedge will thrust forward. In the SR-PP region, the Northern Potwar Deformation Zone (NPDZ), south of the MBT, is assumed to be the back of the wedge, where it is highly deformed. Factors that control the wedge include the taper angle and the yield stress of the weak decollement (Davis et al., 1983). The taper angle of the wedge is made of the basal angle and the topography slope. The topography slope of the Potwar Plateau could be assumed as zero due to the low angle (Lillie et al., 1987). According to Carter and Hansen (1983), the yielding stress of salt is very low and this in turn leads to low topography slope. Moreover, the basal (basement) angle is around 1 degree to 4 degrees which has been confirmed by seismic interpretations (Chapter 3).

In contrast, the Kohat Plateau has a higher topographic slope due to the different detachment layers. Furthermore, according to an InSAR study by Satyabala et al. (2012), the movement of the Kohat Plateau can be equated to a caterpillar. In this model, the plateau moves in blocks of rock, where a block above a weak layer (salt) moves forward and a block that lacks salt is locked due to friction. The block of rock that is locked could accumulate energy and be released as a big earthquake, such as the magnitude 6 earthquake that occurred in 1992 (Satyabala et al., 2012). In order for that to happen, the salt layer underneath the Kohat Plateau needs to have thickness variations, where some blocks are locked and some are moving aseismically (Satyabala et al. 2012). Figure 4.2 shows earthquakes that occurred in the study region from 1973 to 2012. There are no significant earthquakes that occurred in the SR-PP region, which shows that the area has

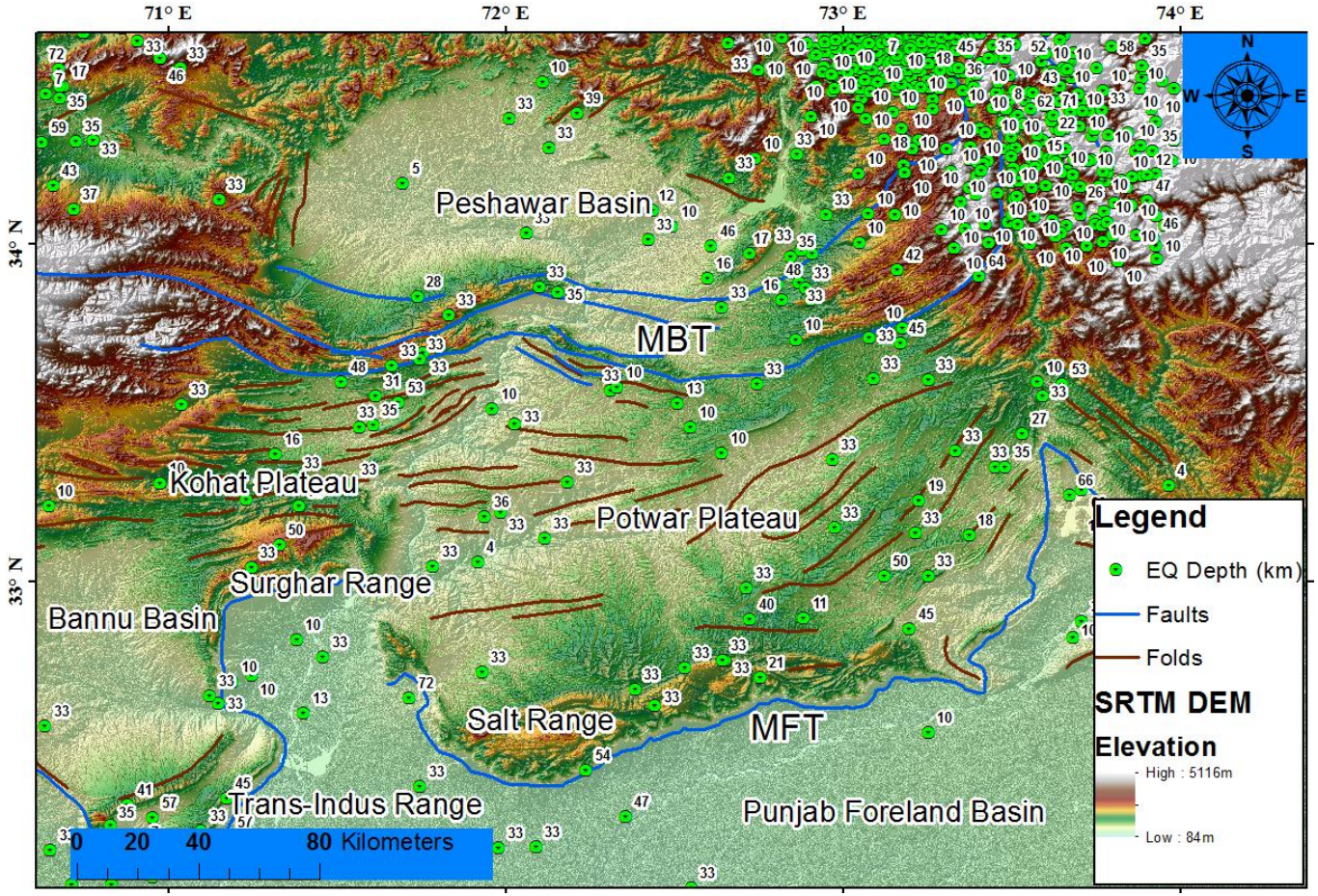

Figure 4.2: Locations of the earthquakes occurred in the study area from 1973 to 2012. The region of Potwar Plateau and Salt Range has a relatively low seismicity with earthquakes of magnitude 5 or less. Most of the earthquakes are deeper than the depth of the salt detachment.

low seismicity. Most of the earthquakes that occurred have magnitude of 5 or less as well as they occurred at depths deeper than the salt decollement (Figure 4.2). This could be attributed to the thick Pre-Cambrian salt layer acting as a decollement, which is shown in our seismic interpretations. Due to the lack of friction between the overburden and the basement rock, most of the Potwar Plateau translated along the detachment without much deformation. Our InSAR and geomorphic index results show that the western SR-PP region and the Main Frontal Thrust (MFT) may still be active, especially in the Salt Range region. Both of the results suggest that the Salt Range region may have undergone uplift from 2007 to 2009. This uplift may be due to a number of factors, which may be salt flow or the compressional forces in the region. However, the area near the Main Boundary Thrust (MBT) is believed to be locked according to GPS studies (Bilham et al., 1997; Bilham, 2004). This could be due to friction, where no there is no weak layer to act as a lubricant. The 'caterpillar' model could also be related to the SR-PP region. Basically, the whole Potwar Plateau may be the block of rock that is moving forward, which is feeding energy to the locked area to the north. This is significant as there are three major cities in the surrounding area, where the population is just over 4 million.

Furthermore, due to the difference in the advance of the Potwar Plateau and the Kohat Plateau, a right-lateral strike-slip fault occurred. Using InSAR, the slip rate of the fault was calculated in a study by Chen and Khan (2010). According to the study, the internal deformation of the Potwar Plateau is more than the deformation at the front of the MFT. However, our results suggest that most of the deformation is concentrated near the MFT, which may be due to a basement offset that uplifted the area.

A model by Treloar et al. (1992), suggested that the Kalabagh fault is an en echelon fault with the Chaman fault, which is the boundary between the Indian plate to the east and the Eurasian plate to the west.

4.1.2 Structural Style of the Central Potwar Plateau Region

2D-seismic interpretation of six commercial seismic lines was shown in chapter 3. The subsurface structural information is essential to understanding the role of salt in the region. Due to the collisional forces between the Indian and the Eurasian plates, this area is still active tectonically. This is proved by our InSAR and geomorphic index results, as well as other studies (Chen and Khan, 2010; Satyabala et al. 2012). However, seismic reflection data can show us how these forces impact the geological structures. Generally, the seismic interpretation results can be summarized as the following:

1) Most of the structural deformation, such as thrust faults and folds are striking east-west. In contrast, little deformation is seen in the east-west profile. This shows that most of the compressional forces are oriented north-south. The general folding that occurs is gentle, symmetrical and can be characterized as low frequency.
2) Most thrust faults that are seen in profiles dips to the north.
3) Normal fault ramps of the basement are related to relatively high deformation above them.
4) The Salt Range Formation (SRF) varies in thickness from 400 meters to 5000 meters. As a consequence, the depth to the salt layer also varies. However, the

depth to the SRF is still more than the 1500 meters threshold, where the salt can overcome the strength of the overburden and start to affect the geological structures.

5) Other than some thrust faults cutting across the overburden layers (molasses section and carbonate platform), they are relatively undeformed and constant in thickness. The carbonate platform, which is the most distinguishable layer in the seismic section, has a constant thickness of 600 meters.

Salt Range Formation (SRF)

The Salt Range Formation was interpreted as the layer between the strong reflectors of carbonate platform and the basement rock. It is evident from the folding of the overburden and the relatively unchanged basement floor that the detachment is located in the SRF which acts as a lubricant between them. As a result of only the overburden propagating southward on the mechanically weak salt layer, this region is categorized as a thin-skinned fold-and-thrust system. Furthermore, it is clear from geological maps and the seismic data that the salt layer did not reach the surface in the Potwar Plateau region. This suggests that the main force that controls the deformation in the Potwar Plateau is the compressional force. Further south towards the Salt Range, salt is exposed and most of the highly deformed structures are concentrated near the MFT suggesting that salt flow may play a significant role towards the south.

Another significant observation is that the depth to the SRF is more that the threshold depth of 1500 meter, where the buoyancy forces of the salt can overcome the

strength of the overburden. According to Hudec and Jackson (2007), the two main forces that drive salt flow are differential loading and buoyancy forces. However, these two forces have to overcome two factors in order for the salt to move upward, which are salt boundary friction and strength of overburden. Furthermore, in order for the buoyancy force to take effect, salt has to be less dense than the surrounding rocks. The salt layer has to be typically around 500 meters to 1600 meters in depth, where the surrounding sedimentary layers are compacted enough to be denser than the salt layer (Hudec and Jackson, 2007). Moreover, the uplift of the Salt Range suggests that the overburden is exposed and eroded, over a long period of time, which leads to the thinning of the overburden. This in turn may lead to buoyancy being the main factor in the salt flow (Figure 4.3). Therefore, we believe that the buoyancy force is the driving mechanism for the salt flow in Salt Range.

In contrast, other than buoyancy force, differential loading could explain the salt movement under the Potwar Plateau. As the basement is dipping to the north, gravity doesn't play a role in the general movement of the salt to the south. There are three types of differential loading; gravitational loading, displacement loading and thermal loading (Hudec and Jackson, 2007). Our model of salt flow in the Potwar Plateau agrees with gravitational loading as the main driving force for the salt (Figure 4.4). Gravitational loading is controlled by the head pressure, where the salt moves from high pressure to low pressure. The head pressure is affected by the thickness (t) of the overburden and the elevation (z) of the salt from an arbitrary datum (Hudec and Jackson, 2007):

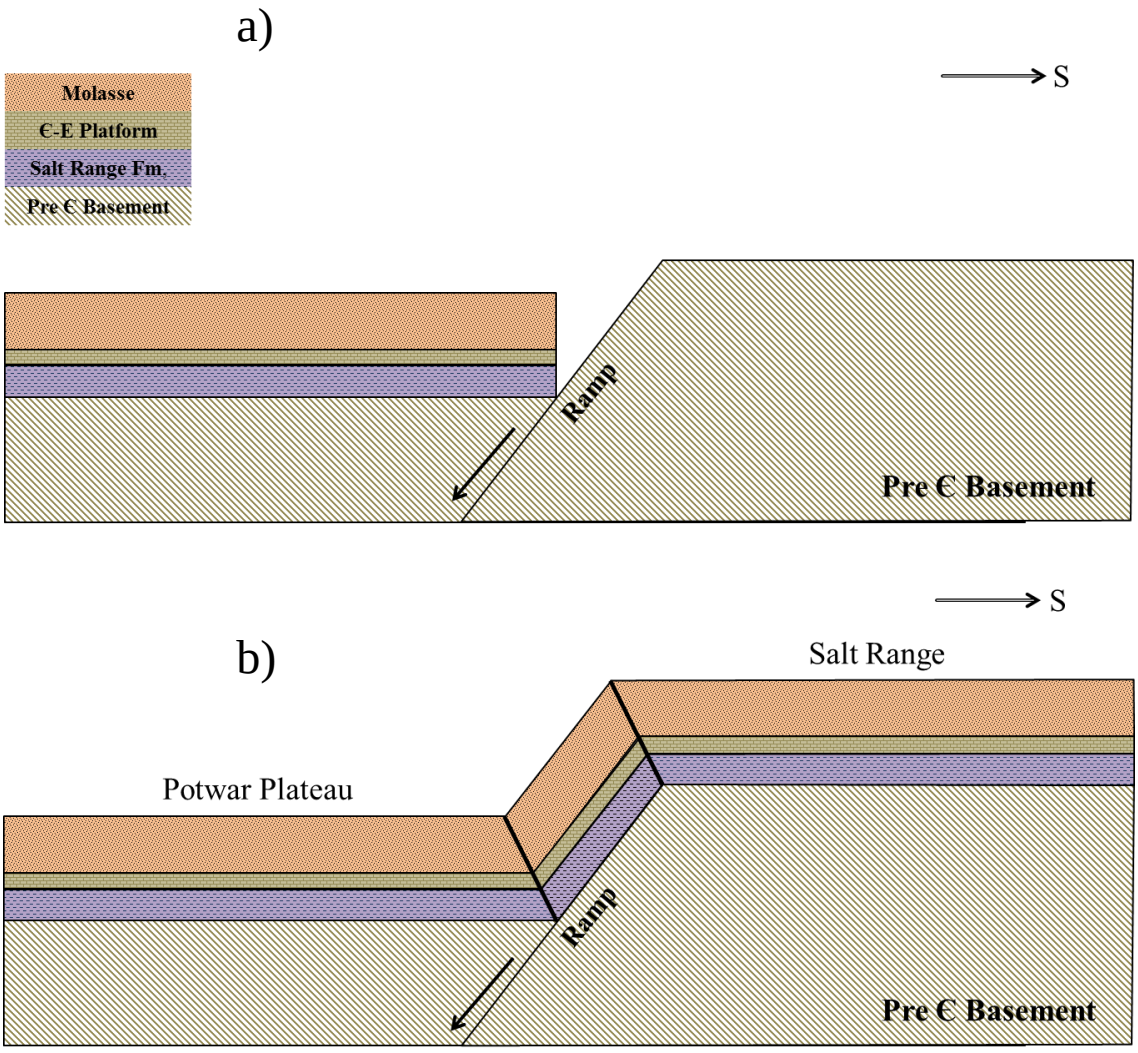

Figure 4.3: A simple model showing the role of the normal fault basement ramp in transitioning between salt decollement at Potwar Plateau and salt flow at the Salt Range. Figure 4.3a refers to before the ramping and Figure 4.3b refers to after the ramping (Modified from Lillie et al., 1987).

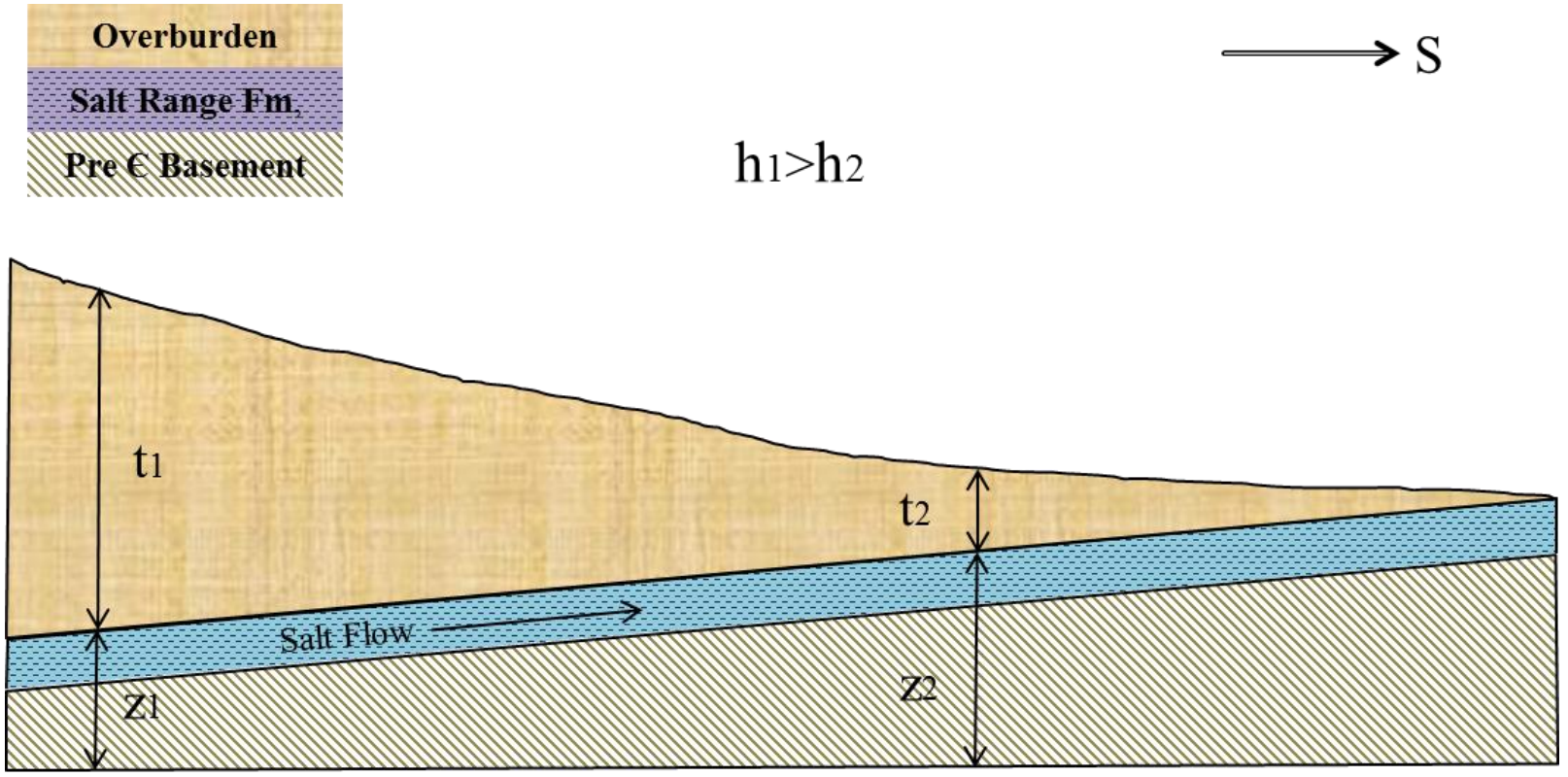

Figure 4.4: A model explaining the gravitational loading. The densities of salt and the overburden are assumed to be constant throughout the whole profile, where the density of the overburden is much higher than the salt. Point 1 has a higher overburden elevation compared to Point 2 (Modified from Hudec and Jackson, 2007).

$$h = z + (\rho_o/\rho_s)\, t$$

In the formula, ρo is the density of the overburden and ρs is the density of the salt. If we assume that both densities are the same for two points along the profile, the flow direction can be predicted (Figure 4.4). At depth, the overburden is denser than the salt layer. Furthermore, the dip of the basement is very small, which is around 1-2 degrees. This suggests that the thickness of the overburden has more influence in the head pressure measurement. Therefore, the salt moves generally to the south due to the head pressure gradient between high pressure to the north and low pressure to the south. In a modeling study by Cotton and Koyi (2000), they discovered that by increasing the thickness of the overburden wedge, the differential load on the salt is increased also increased.

Previous studies have suggested that the Salt Range Formation may have been deposited on the basement rock in a restricted shallow marine environment (Shah, 1977; Bender and Raza, 1995; Jaswal et al., 1997; Wandrey et al., 2004). The salt mainly consists of red salt marls, which are identified as gypsiferous claystones (Shah, 2010). However, other inclusions can also be found in the salt body and these include dolomite, shale and siltstone. These inclusions may be the source for some reflectors in the salt layer as shown in the seismic interpretations.

The seismic interpretations show that the salt thickness varies from 400 meters to 5000 meters. These variations are mostly due to the folding of the overburden. The salt in

synclinal areas will tend to move to anticlinal structures. However, there is not much lateral variation in the thickness of the salt in the Potwar Plateau region. Chen and Khan (2010) show that there is a lateral ramp along the Kalabagh fault that suggest a lateral difference in salt thickness between the Potwar Plateau and the Kohat Plateau. Moreover, Cotton and Koyi (2000) show the importance of lateral thickness of salt in the advance of the plateaus.

Also, there is no evidence of salt to the north near the MBT. The wells that are drilled in this area have not encountered salt. This suggests that either the salt decollement is very deep or the absent. Our model tends to agree with the latter as the area is locked according to previous GPS studies (Bilham et al., 1997; Bilham, 2004).

Normal Fault Basement Ramp

The basement is believed to be of metamorphic nature and is identified as biotite schist (Pennock, 1988). Undulations can be seen on the top surface of the basement and this includes offsets created by normal fault ramps. These ramps may be the cause of uplift in the Salt Range. The overburden and the salt layer are pushed upward and as the Salt Range is eroded, the depth to the salt layer will decrease (Figure 4.3). This in turn will increase the chance of salt flow to affect the deformation. Furthermore, there is also evidence of thrust faults existing at the basement. It is important to note that it is difficult to detect fault planes as being normal or reverse from seismic data alone. There are a number of possible explanations for the existence of the basement ramps. These include normal faulting related to a rifting event in the Pre-Cambrian or Mesozoic period, reverse

faulting due to compressional forces between the Indian and Eurasian plates (Yeats and Hussain, 1987) and lastly, normal faulting due to the southward movement of the overburden (Lillie and Yousuf, 1986). The last explanation is the most accepted reason for the existence of the normal fault ramp.

The normal fault ramp is associated by strong folding with a syncline located above the ramp. This may be due to the ramp acting as a barrier to the southward advance of the plateau before the overburden is pushed over the ramp generating the syncline. This study argues that a normal fault ramp also exists in the western Potwar Plateau. Ground uplift was measured at the north of the DM1 which seems to correspond to folds. A normal fault ramp may exist beneath the folds.

Potential Structural Traps for Hydrocarbon

All of the seismic reflection sections interpreted in this work are commercial lines for the purpose of exploring the region of Potwar Plateau and Salt Range for hydrocarbons. The first commercial discovery of hydrocarbon (1914) in South Asian sub-continent is in the Potwar basin (Akhter et al., 2010). The carbonate platform layer acts as a hydrocarbon reservoir and is the aim for the exploration. Most of the potential hydrocarbon traps in the region are stratigraphic traps and structural traps, which include faulted anticline, pop-up structures and fault blocks (Fazeelat et al., 2010). Some seismic sections show the carbonate platform as anticlines faulted by thrust faults. As the thrust faults displace the carbonate platform, some hydrocarbon may be trapped by the fault plane. These faults may be further disturbed by the salt layer located beneath the

platform. A majority of seals for hydrocarbon traps in the Potwar basin are seals on the hanging wall (Akhter et al., 2010). There could also be traps on the footwall of the fault if the juxtaposing layer is a non-permeable layer, such as shale. Figure 4.5 shows a potential hydrocarbon trap for Line 782-CW-11. The main control on fault seals is the throw of the fault, which varies along the strike of the fault. Therefore, 3-D mapping of the fault will be essential in determining the potential hydrocarbon traps in this region. In contrast to the Potwar basin, salt is located above the reservoir rocks in the Gulf of Mexico, where salt can act as a seal as well as creates different salt traps.

4.1.3 Salt Decollement vs. Salt Flow

This study follows the approach of backward modeling, where the study area is first mapped with geophysical and geological data. Afterwards, a model is suggested from the acquired data. From the data acquired, our model suggests that the normal basement ramp is transitioning the role of salt from north to south. The salt layer acts as a decollement for the Potwar Plateau region and salt flow becomes prominent in the Salt Range. Furthermore, our results suggests that the same mechanism can be applied to the west SR-PP. Due to the possible uplift of the Salt Range and the existence of salt exposure near the MFT, a basement ramp may be a reasonable explanation. Future seismic imaging of the western Potwar Plateau may give a better constraint of the subsurface.

Furthermore, the results from this thesis suggest that the moving mechanism for the SR-PP is closely related to the wedge model. Seismic interpretation shows that the

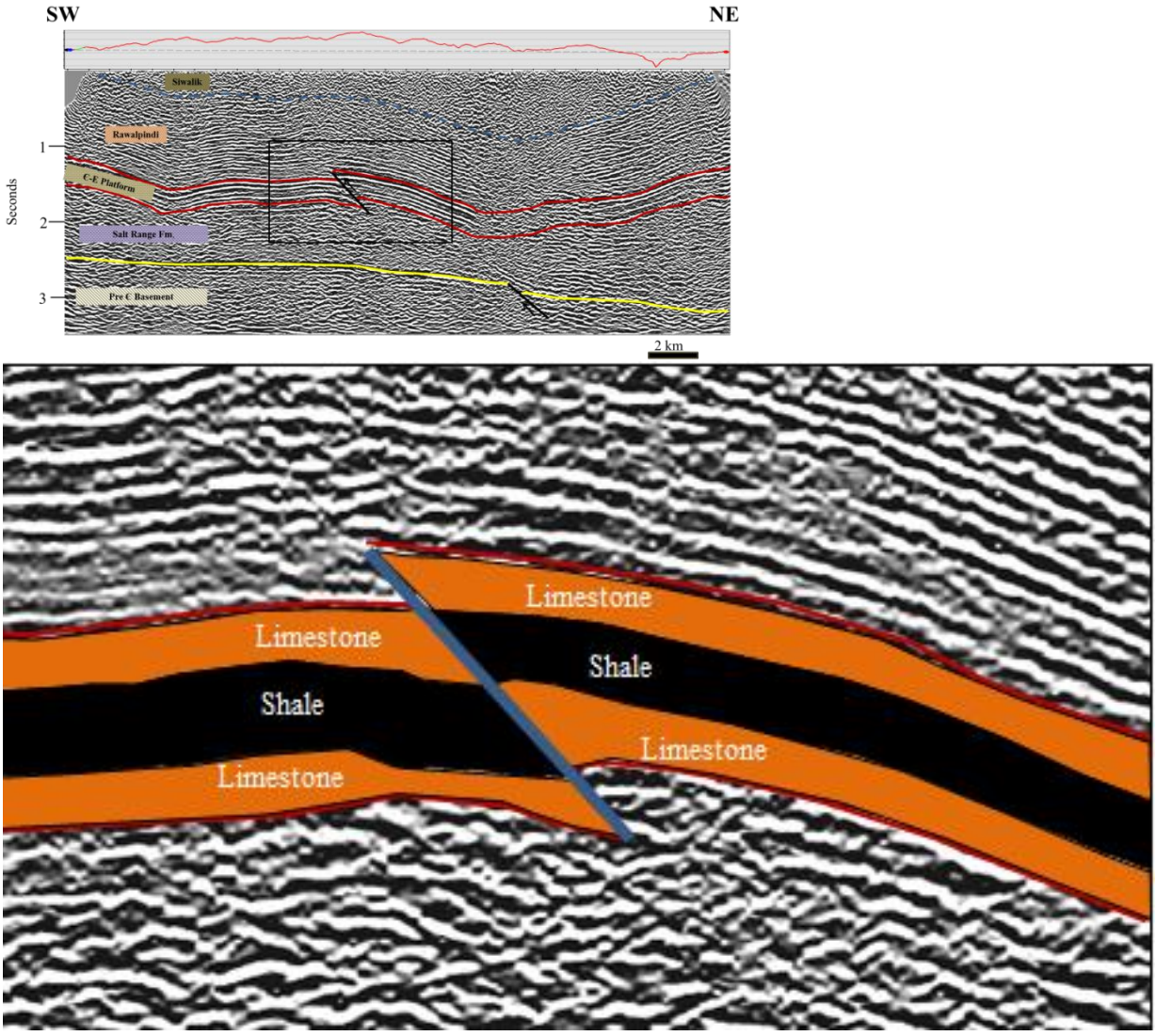

Figure 4.5: An example of a potential hydrocarbon trap for Line 782-CW-11. The carbonate platform is displaced by a thrust fault. Both the hanging wall and the footwall have seals by non-permeable shale layer.

Salt Range Formation acts as a decollement due to its weak nature. Therefore, this study concludes that the thickness of the salt is important in the movement of the wedge. Thicker salt layer will result in lower yielding stress and will lead to lower taper angle, which is seen in the Potwar Plateau. In contrast, the Kohat Plateau has a higher taper angle due to the friction between the overburden and the lower layers. Therefore, this thesis suggests that the SR-PP is a thin-skinned fold-and-thrust belt.

Even though the salt layer is essential in the deformation style in this region, the condition of the basement is also important. It is evident that the uplift in the Salt Range could be mainly due to the basement ramp. This uplift may cause the overburden to weaken through erosion and salt flow deformation to occur. Therefore, both the salt and the condition of the basement affect the deformation in the Salt Range and Potwar Plateau region.

4.2 Conclusions

The Salt Range-Potwar Plateau is an ideal and interesting region to study salt tectonics. Many studies have studied this region in relation to the adjacent Kohat Plateau due to the clear difference in deformation between the two systems. Salt tectonic studies in this region are essential to understand the powerful forces that control the difference in deformations. Other than a potential area for oil and gas discoveries, this study may help in understanding the earthquake potential in this region.

Both InSAR and seismic data are two very different datasets and both are utilized in this study. Furthermore, both of these data gave different views of this region. While InSAR shows the movements of the region, the seismic data displays how those movements deformed the subsurface. Additionally, the mountain-front sinuosity index shows that the Salt Range may have undergone uplift. Most of the deformation in this region can be related to salt due to its weak nature. This thesis suggests that the wedge model explains the movement of the SR-PP region. Additionally, the 'caterpillar' model can also explain the potential earthquake near the MBT. Both models explain the movement of the SR-PP region from different perspective. On one hand, the 'caterpillar' model looks at the movement on a larger scale; the wedge model is on a smaller scale. Moreover, the existence of basement ramps due to normal faults can be seen in seismic interpretations. These basement ramps act as transition zones for the roles of salt in the north and the south. Our study shows that the salt layer acts as a decollement in the Potwar Plateau region, while salt flows are prominent in the Salt Range. Therefore, both the existence of salt and the condition of the basement affect the deformation style of this region.

Finally, we find that differential loading may be the main driving force for the salt to the south. On the other hand, buoyancy is the driving force for the Salt Range area.

REFERENCES

Abbasi, I. A., McElroy, R. 1991. Thrust kinematics in Kohat Plateau, Trans Indus Range, Pakistan. Journal of Structural Geology, 13(3), 319-327.

Aftabi, P., Roustaie, M., Alsop, G. I., Talbot, C. J. 2010. InSAR mapping and modeling of an active Iranian salt extrusion. Journal of the Geological Society, London, 167, 155-170.

Akhter, G., Ahmad, Z., Munir, M. Z. 2010. Fault seal analysis indicates potential of Paleogene reservoirs in Pakistan. Oil & Gas Journal, 108(11), 34-42.

Baker, D. M., Lillie, R. J., Yeats, R. S., Johnson, G. D., Yousuf, M., Zamin, A. S. H. 1988. Development of the Himalayan frontal thrust zone: Salt Range, Pakistan. Geology, 16, 3-7.

Bayuaji L., Sri Sumantyo, J. T., Kuze, H. 2010. ALOS PALSAR D-InSAR for land subsidence mapping in Jakarta, Indonesia. Canadian Journal of Remote Sensing, 36(1), 1-8.

Bilham, R. 2004. Earthquakes in India and the Himalaya: tectonics, geodesy and history. Annals of Geophysics, 47 (2/3), 839-858.

Bilham, R., Larson, K., Freymueller, J. 1997. GPS measurements of present-day convergence across the Nepal Himalaya. Nature, 386, 61-64.

Buckley, S. M., Rosen, P. A., Hensley, S., Tapley, B. D. 2003. Land subsidence in Houston, Texas, measured by radar interferometry and constrained by extensometers. Journal of Geophysics Research 108(B11), 2542, doi:10.1029/2002JB001848.

Bull, W. B. and McFadden, L. D. 1977. Tectonic geomorphology north and south of the Garlock fault, California. In D. O. Doehring (ed.), Geomorphology in Arid Regions. Proceedings of the Eighth Annual Geomorphology Symposium. Binghamton, NY: State University of New York at Binghamton, 115-138.

Carter, N. L. and Hansen, F. D. 1983. Creep of rocksalt. Tectonophysics, 92(N4), 275-333.

Chang, W. L., Smith, R. B., Farrell, J., Puskas, C. M. 2010. An extraordinary episode of Yellowstone caldera uplift, 2004-2010, from GPS and InSAR observations. Geophysical Research Letters, 37, L23302.

Chapple, W. M. 1978. Mechanics of thin-skinned fold-and-thrust belts. Geological Society of America Bulletin, 89(8), 1189-1198.

Chen, L. 2009. Application of remote sensing techniques to study the Neotectonics in the Northwestern Himalayan fold-and-thrust belt, Pakistan. Thesis. University of Houston.

Chen, L., Khan, S. D. 2010. InSAR observation of the strike-slip faults in the northwest Himalayan frontal thrust system. Geosphere, 6, 731-736.

Closson, D., Karaki, N. A., Milisavljevic, N., Hallot, F., Acheroy, M. 2011. Salt Tectonics of the Lisan Diapir revealed by synthetic aperture radar images. Tectonics, Dr. Damien Closson (Ed.), ISBN: 978-953-307-545-7, pg. 303-328.

Cotton, J. T., Koyi, H. A. 2000. Modeling of thrust fronts above ductile and frictional detachments: Application to structures in the Salt Range and Potwar Plateau, Pakistan. Geological Society of America Bulletin, 112(3), 351-363.

Curlander, J. C., McDonough, R. N. 1991. Synthetic Aperture Radar Systems and Signal Processing. Wiley-Interscience, Tororonto, Ont.

Davis, D. M., Engelder, T. 1985. The role of salt in fold-and-thrust belts. Tectonophysics, 119, 67-88.

Davis, D., Suppe, J., Dahlen, F. A. 1983. Mechanics of fold-and-thrust belts and accretionary wedges. Journal of Geophysical Research, 88(B2), 1153-1172.

ENVI. 2010. Exploring the SARscape Module for ENVI. ITT Visual Information Solutions.

Fazeelat, T., Jalees, M. I., Bianchi, T. S. 2010. Source rock potential of Eocene, Paleocene and Jurassic deposits in the subsurface of the Potwar basin, Northern Pakistan. Journal of Petroleum Geology, 33(1), 87-96.

Funning, G. J., Parsons, B., Wright, T. J. 2007. Fault slip in 1997 Manyi, Tibet earthquake from linear elastic modeling if InSAR displacements. Geophys. J. Int., 169, 988-1008.

Goldstein, R. M. and Werner, C. L. 1998. Radar interferogram filtering for geophysical applications. Geophysical Research Letters, 25(21), 4035-4038.

Grelaud, S., Sassi, W., Frizon de Lamotte, D., Jaswal, T., Roure, F. 2002. Kinematics of eastern Salt Range and South Potwar Basin (Pakistan): a new scenario. Marine and Petroleum Geology, 19, 1127-1139.

Hodges, K. V. 2000. Tectonic of the Himalaya and southern Tibet from two perspectives. Geological Society of America Bulletin, 112(3), 324-350.

Hooper, A., Zebker, H., Segall, P., Kampes, B. 2004. A new method for measuring deformation on volcanoes and other natural terrains using InSAR persistent scatterers. Geophysical Research Letters, 31(L23611), 1-5.

Hudec, M. R. and Jackson, M. P. A. 2007. Terra infirma: Understanding salt tectonics. Earth-Science Reviews, 82(1-2), 1-28.

Jackson, M. P. A. 1995. Retrospective salt tectonics. AAPG Memoir, 65, 1-28.

Jade, S., Rao, H. J. R., Vijayan, M. S. M., Gaur, V. K., Bhatt, B. C., Kumar, K., Jaganathan, S., Ananda, M. B., Kumar, P. D. 2011. GPS-derived deformation rates in northwestern Himalaya and Ladakh. Int. J. Earth Sci, 100, 1293-1301.

Jaume, S. C. 1986. The Mechanics of the Salt Range-Potwar Plateau, Pakistan: Qualitative and Quantitative Aspects of a Fold-and-Thrust Belt Underlain by Evaporites. MS Thesis. Oregon State University.

Jaume, S. C., Lillie, R. J. 1988. Mechanics of the Salt Range-Potwar Plateau, Pakistan: A fold-and-thrust belt underlain by evaporites. Tectonics, 7(1), 57-71.

Kaneda, H., Nakata, T., Tsutsumi, H., Kondo, H., Sugito, N., Awata, Y., Akhtar, S. S., Majid, A., Khattak, W., Awan, A. A., Yeats, R. S., Hussain, A., Ashraf, M., Wesnousky, S. G., Kausar, A. B. 2008. Surface rupture of the 2005 Kashmir, Pakistan, earthquake and its active tectonic implications. Bulletin of the Seismological Society of America, 98(2), 521-557.

Keller, E. A. and Pinter, N. 2002. Active Tectonics: Earthquakes, Uplift, and Landscape. Prentice Hall, 2nd ed. 362 pg.

Khan, M. A., Bendick, R., Bhat, M. I., Bilham, R., Kakar, D. M., Khan, S. F., Lodi, S. H., Qazi, M. S., Singh, B., Szeliga, W., Wahab, A. 2008. Preliminary geodetic

constraints on plate boundary deformation on the western edge of the Indian plate from TriGGnet (Tri-University GPS Geodesy Network). Journal of Himalayan Earth Sciences, 41, 71-87.

Khan, S. D., Chen, L., Ahmad, S., Ahmad, I., Ali, F. 2012. Lateral structural variation along the Kalabagh Fault Zone, NW Himalayan foreland fold-and-thrust, Pakistan. Journal of Asian Earth Sciences, 50, 79-87.

Kozary, M. T., Dunlap, J. C., Humphrey, W. E. 1968. Incidence of saline deposits in geologic time. Spec. Pap. Geological Society Am., 88, 43-57.

Leathers, M. R. 1987. Balanced Structural Cross Section of the Western Salt Range and Potwar Plateau, Pakistan: Deformation Near the Strike-Slip Terminus of an Overthrust Sheet. MS Thesis. Oregon State University.

Li, Z. W., Ding, X. L., Huang, C., Zou, Z. R., Chen, Y. L. 2007. Atmospheric effects on repeat-pass InSAR measurements over Shanghai region. Journal of Atmospheric and Solar-Terrestrial Physics, 69, 1344-1356.

Lillie, R. J., Johnson, G. D., Yousuf, M., Zamin, A. S. H., Yeats, R. S. 1987. Structural development within the Himalayan foreland fold-and-thrust belt of Pakistan. Canadian Society of Petroleum Geologists, Memoir 12, 379-392.

Lubis, A. M., Sato, T., Tomiyama, N., Isezaki, N., Yamanokuchi, T. 2011. Ground subsidence in Semarang-Indonesia investigated by ALOS-PALSAR satellite SAR interferometry. Journal of Asian Earth Sciences, 40, 1079-1088.

Massonet, D., Feigl, K. L. 1995. Discriminating geophysical phenomena in satellite radar interferograms. Geophysical Research Letters, 22(12), 1537-1540.

Massonnet, D., Feigl, K. L. 1998. Radar interferometry and its application to changes in the earth's surface. Reviews of Geophysics, 36(4), 441-500.

McDougall, J. W., Khan, S. H. 1990. Strike-slip faulting in a foreland fold-thrust belt: the Kalabagh fault and western salt range, Pakistan. Tectonics, 9(5), 1061-1075.

Motagh, M., Djamour, Y., Walter, T. R., Wetzel, H. U., Zschau, J., Arabi, S. 2007. Land subsidence in Mashhad Valley, northeast Iran: results from InSAR, leveling and GPS. Geophy. J. Int., 168, 518-526.

Ni, J. F. 1989. Active tectonics of the Himalaya. Proc. Indian Acad. Sci. (Earth Planet Sci.), 98(1), 71-89.

Pennock, E. S. 1988. Structural Interpretation of Seismic Reflection Data from the Eastern Salt Range and Potwar Plateau, Pakistan. MS Thesis. Oregon State University.

Pivnik, D. A. 1992. Depositional response to encroachment of Himalayan compressional and transpressional deformation on the northern Pakistan foreland. MS Thesis. Dartmouth College, Hanover, New Hampshire, 329 pg.

Qayyum, M. 1991. Crustal Shortening and Tectonic Evolution of the Salt Range in Northwest Himalaya, Pakistan. MS Thesis. Oregon State University.

Reigber, A. and Moreira, J. 1997. Phase unwrapping by fusion of local and local methods. Geoscience and Remote Sensing, 1997. IGARSS '97. Remote Sensing - A Scientific Vision for Sustainable Development., 1997 IEEE International, 2, 869-871.

Robion, P., Grelaud, S., Frizon de Lamotte, D. 2007. Pre-folding magnetic fabrics in fold-and-thrust belts: Why the apparent internal deformation of the sedimentary rocks from the Minervois basin (NE — Pyrenees, France) is so high compared to the Potwar basin (SW — Himalaya, Pakistan)? Sedimentary Geology, 196, 181-200.

Samsonov, S. V. 2007. Integration of Differential InSAR and GPS measurements for studying of surface deformation. MS Thesis. University of Western Ontario.

Satyabala, S.P., Yang, Z., Bilham, R. 2012. Stick-slip advance of the Kohat Plateau in Pakistan. Nature Geoscience, 5, 147-150.

Sefercik, U. G., Dana, I. 2011. Crucial points of interferometric processing for DEM generation using high resolution SAR data. ISPRS Hannover Workshop 2011: High-resolution earth imaging for geospatial information, Volume XXXVIII-4/W19

Sercombe, J. W., Pivnik, D. A., Wilson, W. P., Albertin, M. L., Beck, R. A., Stratton, M. A. 1998. Wrench faulting in the Northern Pakistan Foreland. AAPG Bulletin, 82(11), 2003-2030.

Sommaruga, A. 1999. Decollement tectonics in the Jura foreland fold-and-thrust belt. Marine and Petroleum Geology, 16, 111-134.

Talbot, C. J. 1992. Quo vadis tectonophysics? With a pinch of salt! J. Geodynamics, 16(1/2), 1-20.

Thakur, V. C. 2004. Active tectonics of Himalayan Frontal Thrust and seismic hazard to Ganga Plain. Current Science, 86(11), 1554-1560.

Treloar, P. J., Coward, M. P., Chambers, A. F., Izatt, C. N., Jackson, K. C. 1992. Thrust geometries, interferences and rotations in the northwest Himalaya. In: McClay, K. R. (Ed.), Thrust Tectonics. Chapman and Hall, London, pp. 325-342.

Utley, J. A. 2004. Using InSAR and GPS to detect ground subsidence in Pahrump Valley. MS Thesis. University of Nevada, Reno.

Wakabayashi, H., Ito, N., Hamazaki, T. 1998. PALSAR System on the ALOS. SPIE Proceedings Series, 3498, 181-189.

Wang, H., Wright, T. J., Biggs, J. 2009. Interseismic slip rate of the northwestern Xianshuihe fault from InSAR data. Geophysical Research Letters, 36, L03302.

Wesnousky, S. G., Kumar, S., Mohindra, R., Thakur, V. C. 1999. Uplift and convergence along the Himalayan Frontal Thrust of India. Tectonics, 18(6), 967-976.

Weston, J., Ferreira, A. M. G., Funning, G. J. 2012. Systematic comparisons of earthquake source models determined using InSAR and seismic data. Tectonophysics, 532-535, 61-81.

Wright, T. J., Parsons, B., England, P. C., Fielding, E. J. 2004. InSAR observations of low slip rates on the major faults of Western Tibet. Science, New Series, 305(5681), 236-239.

Yeats, R. S., Khan, S. H., Akhta, M. 1984. Late Quaternary deformation of the Salt Range of Pakistan. Geological Society of America Bulletin, 95, 958-966.

Yeats, R. S., Lillie, R. J. 1991. Contemporary tectonics of the Himalayan frontal fault system: folds, blind thrusts and 1905 Kangra earthquake. Journal of Structural Geology, 13(2), 215-225.

Yin, A. 2006. Cenezoic tectonic evolution of the Himalayan orogeny as constrained by along-strike variation of structural geometry, exhumation history, and foreland sedimentation. Earth-Science Reviews, 76, 1-131.

Yin, A. and Harrison, T. M. 2000. Geological evolution of the Himalayan Tibetan orogeny. Annual Review of Earth and Planetary Sciences, 28, 211-280.